JOURNAL OF NEUROPHYSIOLOGY
Vol. 66, No. 5, November 1991. Printed in U.S.A.

Control of Orienting Gaze Shifts by the Tectoreticulospinal System in the Head-Free Cat. III. Spatiotemporal Characteristics of Phasic Motor Discharges

DOUGLAS P. MUNOZ, DANIEL GUITTON, AND DENIS PÉLISSON
Montreal Neurological Institute and Department of Neurology and Neurosurgery, McGill University, Montreal, Quebec H3A 2B4, Canada

SUMMARY AND CONCLUSIONS

1. In this paper we describe the movement-related discharges of tectoreticular and tectoreticulospinal neurons [together called TR(S)Ns] that were recorded in the superior colliculus (SC) of alert cats trained to generate orienting movements in various behavioral situations; the cats' heads were either completely unrestrained (head free) or immobilized (head fixed). TR(S)Ns are organized into a retinotopically coded motor map. These cells can be divided into two groups, fixation TR(S)Ns [fTR(S)Ns] and orientation TR(S)Ns [oTR(S)Ns], depending on whether they are located, respectively, within or outside the zero (or area centralis) representation of the motor map in the rostral SC.

2. oTR(S)Ns discharged phasic motor bursts immediately before the onset of gaze shifts in both the head-free and head-fixed conditions. Ninety-five percent of the oTR(S)Ns tested (62/65) increased their rate of discharge before a visually triggered gaze shift, the amplitude and direction of which matched the cell's preferred movement vector. For movements along the optimal direction, each cell produced a burst discharge for gaze shifts of all amplitudes equal to or greater than the optimum. Hence, oTR(S)Ns had no distal limit to their movement fields. The timing of the burst relative to the onset of the gaze shift, however, depended on gaze shift amplitude: each TR(S)N reached its peak discharge when the instantaneous position of the visual axis relative to the target (i.e., instantaneous gaze motor error) matched the cell's optimal vector, regardless of the overall amplitude of the movement.

3. The intensity of the movement-related burst discharge depended on the behavioral context. For the same vector, the movement-related increase in firing was greatest for visually triggered movements and less pronounced when the cat oriented to a predicted target, a condition in which only 76% of the cells tested (35/46) increased their discharge rate. The weakest movement-related discharges were associated with spontaneous gaze shifts.

4. For some oTR(S)Ns, the average firing frequency in the movement-related burst was correlated to the peak velocity of the movement trajectory in both head-fixed and head-free conditions. Typically, when the head was unrestrained, the correlation to peak gaze velocity was better than that to either peak eye or head velocity alone.

5. Gaze shifts triggered by a high-frequency train of collicular microstimulation had greater peak velocities than comparable amplitude movements elicited by a low-frequency train of stimulation.

6. A visually or stimulation-induced burst of oTR(S)N discharge imposed in the middle of a gaze shift caused a short-latency reacceleration of both the eyes (~10 ms) and head (~25 ms). The modified gaze saccade terminated with the visual axis aligned on the target.

7. fTR(S)Ns reduced their rate of discharge when the cat generated orienting gaze shifts with the head fixed or free. These cells resumed their sustained discharge when the gaze shifts terminated with the visual axis aligned on the target (i.e., zero gaze motor error).

8. These observations suggest that instantaneous gaze motor error was topographically coded in the TR(S)N layer of the cat's SC. At the start of an orienting gaze shift, a zone of activity was established at the collicular locus that coded the desired gaze displacement. As the gaze shift proceeded, this zone of TR(S)N activity moved continuously across the SC motor map, toward the zero representation in the rostral pole. Its instantaneous location specified the remaining gaze motor error. As the gaze shift terminated, the active zone invaded the rostral poles, where fTR(S)Ns are located.

9. We propose that TR(S)Ns lie within a gaze feedback loop that controls eye-head orienting movements via inputs onto selected elements within the brain stem premotor circuitry. In particular, we postulate that oTR(S)Ns project preferentially on long-lead burst neurons, whereas fTR(S)Ns, located in the rostral pole of the SC, project predominantly onto omnipause neurons (OPNs). During an orienting gaze shift, the feedback of change in gaze position would cause the active zone to move across the TR(S)N layer of the SC, and fTR(S)N-induced activation of OPNs would stop the movement.

INTRODUCTION

The preceding two papers (Guitton and Munoz 1991; Munoz and Guitton 1991) showed that efferent neurons of the cat superior colliculus (SC), tectoreticular neurons (TRNs), and tectoreticulospinal neurons (TRSNs) [together called TR(S)Ns] carry both sensory and anticipatory signals relevant to the control of orienting behavior. During periods when the visual axis is stationary, the locus of TR(S)N activity on the collicular motor map specifies gaze position error (i.e., the difference between current and desired positions of the visual axis). A zone of sustained activity (point image), corresponding to a single target of interest, changes position on the map as the cat fixates different points in space relative to the target. When the cat fixates the target itself, gaze position error equals 0, and fixation TR(S)Ns [fTR(S)Ns], located in the rostral pole of the SC, are activated, whereas TR(S)Ns located elsewhere on the SC motor map are at a reduced level of excitability. The sustained activity emanating from these

fTR(S)Ns may have a suppressive effect on the generation of orienting movements (Munoz and Guitton 1991). When the animal subsequently looks away from the target, the zone of sustained activity shifts to a new collicular site representing the current gaze position error vector. We postulated that these latter cells are involved via their sustained discharge in motor preparation and referred to them as orientation TR(S)Ns [oTR(S)Ns], because their activation increases the probability that an orienting movement will be made to the target. In this paper we show that oTR(S)Ns also participate directly in commanding an eye-head orienting movement. They do this via the action of a phasic burst for which the characteristics and links with the eye, head, and gaze (= position of visual axis in space = eye-in-head + head-in-space) trajectories are discussed.

Several studies have described motorlike discharge patterns of neurons in the deeper layers of the monkey SC. For example, saccade-related burst neurons (SRBNs) discharge a burst of spikes before saccadic eye movements of the appropriate amplitude and direction (Schiller and Koerner 1971; Sparks 1978; Sparks et al. 1976; Sparks and Mays 1980; Wurtz and Goldberg 1971, 1972a). It has always been assumed that this class of neuron forms the motor command output pathway from the SC to the eye premotor circuits. To date, only a few studies have attempted to confirm this by recording the activity of collicular output neurons in alert animals (Berthoz et al. 1986; Grantyn and Berthoz 1985; Keller 1979; Moschovakis et al. 1988b; Munoz 1988; Munoz and Guitton 1986, 1989). Although the discharge of these neurons is considerably more complex than hitherto suspected, the results suggest that TR(S)Ns carry at least part of the presaccadic signal.

Sparks and Mays (1981) suggested that the SRBN provides the brain stem with a trigger that initiates the saccade. In the classical view of this system, the locus of discharge in the SC specifies saccade amplitude and direction. The frequency of discharge in the burst was originally thought not to affect saccade velocity. However, recent evidence suggests that the SC, in addition to its role in determining the movement vector, may also play a role in controlling the acceleration and velocity of ocular saccades (Berthoz et al. 1986; Hikosaka and Wurtz 1985, 1986; Lee et al. 1988; Munoz and Guitton 1986, 1989; Rohrer et al. 1987; Waitzman et al. 1988).

In the cat, the latency, velocity, and acceleration of both eye and head orienting movements covary, thereby suggesting that the eye and head motor systems share a common drive (Guitton et al. 1990). This common signal may be provided, at least in part, by oTR(S)Ns, because they distribute collaterals to several brain stem regions implicated in oculomotor and head motor control (Grantyn and Grantyn 1982). To date, only a few studies utilizing either the cat (Harris 1980; Peck 1990; Straschill and Schick 1977) or primate (Robinson and Jarvis 1974) have described single-unit recordings of cells in the SC of animals with the head unrestrained. Because of this very limited amount of data, none of the reported observations have yielded significant insight into how neural elements within the colliculus may be involved in gaze control. However, other lines of experimentation have suggested that the deeper layers of the cat SC are critical for the generation of coordinated eye-head orienting movements. Microstimulation of the deeper laminae of the cat SC elicits coordinated eye and head orienting movements (Hess et al. 1946; Roucoux et al. 1980; Syka and Radil-Weiss 1972), the organization of which appears to be based on principles similar to those of naturally occurring eye-head orienting movements (Guitton et al. 1984, 1990). The amplitudes and directions of the evoked gaze displacements are determined by the position of activity on the motor map (Crommelinck et al. 1990; Roucoux et al. 1980).

In this paper, we describe the activity of TR(S)Ns located throughout the SC when trained cats generated either eye movements while their heads were immobilized (head fixed) or coordinated eye-head orienting movements while their heads were unrestrained (head free). We will first describe the movement-related phasic discharges of oTR(S)Ns, illustrating how behavioral context influences this activity. We will also consider how these discharge patterns contribute to the coding of eye and head movement latency and velocity. Then we will describe the time-varying spatial distribution of TR(S)N activity on the SC motor map during the execution of orienting gaze shifts. It will be demonstrated that, as the visual axis moves toward the target of interest, there is a continuous shift toward the fixation zone in the topographical distribution of TR(S)N burst activity within the SC. We propose that the SC resides inside a gaze feedback loop and that TR(S)Ns provide the brain stem premotor circuitry with a spatially coded instantaneous gaze motor error signal.

Preliminary reports of some of these observations have appeared elsewhere (Munoz and Guitton 1986, 1989; Munoz et al. 1991).

METHODS

Experimental procedures

In this paper we describe the movement-related discharges of TR(S)Ns that were recorded in different behavioral paradigms. Refer to Guitton et al. (1990) for general methods employed in preparing cats for chronic recordings and in measuring eye, head, gaze, and target displacements; to Guitton and Munoz (1991) for procedures used in identifying and recording TR(S)N activity; and to Munoz and Guitton (1991) for behavioral techniques. Recordings were made when the head was held immobilized or completely unrestrained.

It was possible to elicit both visually triggered and predictive orienting movements from alert cats (Guitton et al. 1990; Munoz and Guitton 1991). Movements to a predicted target were evoked when a food target was moved from one side of an opaque barrier to behind and the animal, anticipating target reappearance, oriented to the other side. Visually triggered movements were elicited when the food target suddenly appeared at one edge of the barrier. Barrier width and orientation were varied to have the animal generate gaze shifts of various amplitudes and directions. To increase the range of movement amplitudes sampled, we centered the barrier in front of the animal so that the two edges of interest were situated on either side of center.

In a typical experiment, once a TR(S)N was isolated, a barrier was chosen such that when the cat looked to one side, the opposite edge was within the gaze position error field of the cell under study and the vector (i.e., amplitude and direction) of movement required to shift the visual axis to the closest point on the opposite edge of this barrier corresponded to the cell's optimal gaze position

error vector (Munoz and Guitton 1991). We recorded neural activity while the animal generated several predictively and visually triggered gaze shifts of this amplitude and direction, in both head-free and head-fixed conditions. Then, if the unit was still well isolated, we placed other barriers in front of the cat and recorded neural activity associated with gaze shifts of other amplitudes and directions.

Microstimulation of the SC

During experiments, the SC was routinely microstimulated to elicit orienting gaze shifts or to modify the trajectories of ongoing movements. Trains of current-regulated pulses (0.5-ms pulse duration) were delivered through either the glass micropipette or a microwire. Very low current strengths (5–30 μA) were required to generate orienting movements when stimulation was confined to the layers of the SC containing TR(S)Ns. Threshold current was defined as the current required to elicit movement on 50% of the train presentations. The frequency of pulses within a train of stimuli and the duration of the train were varied considerably. Stimulation parameters will be provided in the RESULTS as they pertain to specific experiments.

Data analysis

The movement-related discharge patterns of TR(S)Ns were evaluated both qualitatively and quantitatively. Qualitative analyses consisted of displaying TR(S)N rasters and histograms in association with gaze, head, and eye position and velocity trajectories. The different approaches used to quantitatively compare aspects of TR(S)N discharge with movement parameters are described below.

CALCULATION OF AVERAGE FIRING FREQUENCY AND DETERMINATION OF MOVEMENT FIELDS. We calculated the average phasic firing frequency of an oTR(S)N as a measure of the intensity of a cell's movement-related discharge during the occurrence of an orienting gaze shift. Because electrical stimulation of the SC during an ongoing movement causes an acceleration of gaze 10 ms later (see Fig. 6 and Table 1) and an oTR(S)N burst discharge could reaccelerate gaze within 10 ms (see Fig. 4 and Table 1), the number of action potentials recorded in an interval spanning from 10 ms before onset of the movement to 10 ms before its termination was divided by the corresponding time interval to produce an average firing frequency. The average firing frequency was compared with the maximum gaze, eye, and head velocities in an orienting movement (e.g., see Fig. 3).

Movement fields are three-dimensional polar plots showing the number of spikes in a burst versus movement amplitude and direction (Sparks et al. 1976; Wurtz and Goldberg 1972a). We quantitatively determined the movement fields of oTR(S)Ns, by counting the number of action potentials recorded in the interval between 10 ms before onset of each single-step gaze saccade and 10 ms before its termination. In this analysis, only predictively triggered movements were considered, because, as we shall see, this avoided phasic visual responses that would have contaminated the phasic movement-related neuronal activity. In each movement direction, the spike count was plotted against movement amplitude for each of the eye, head, and gaze trajectories.

CALCULATION OF SPIKE PROBABILITY DENSITY FUNCTION. To obtain an estimate of the probability of occurrence of an action potential, it is usual to sum many responses into histograms that give an estimate of the probability of spike occurrence in each bin. To improve this estimate, we substituted Gaussians (20 ms wide) for each spike to produce a continuous function (spike probability function) that represented the probability of spike occurrence (Richmond et al. 1987; Silverman 1986; Waitzman et al. 1988).

TABLE 1. *Latency from onset of oTR(S)N or microstimulation burst to reacceleration of gaze, eye, and head*

	Gaze, ms	Eye, ms	Head, ms
Cell			
H1	9 ± 1 (7)	9 ± 1 (7)	29 ± 2 (7)
Q9	9 ± 2 (5)	9 ± 2 (5)	24 ± 3 (5)
Q24	11 ± 4 (18)	10 ± 4 (16)	24 ± 6 (16)
Q37	8 ± 2 (3)	8 ± 2 (3)	32 ± 3 (3)
Q55	10 ± 4 (13)	10 ± 4 (13)	34 ± 5 (9)
Q62	12 ± 3 (5)	12 ± 3 (5)	31 ± 4 (4)
Average	10 ± 1 (6)	10 ± 1 (6)	29 ± 4 (6)
Stimulation			
Cat J	11 ± 4 (8)	11 ± 4 (8)	24 ± 4 (6)
Cat S	10 ± 4 (12)	10 ± 4 (12)	23 ± 5 (12)

Values are means ± SD; number of observations in parentheses. oTRSN, orientation tectoreticulospinal neuron.

This function was used only to discern a peak in a discharge profile and to plot a discharge profile as a continuous function. The sum of many transformed spike trains is the average spike density function.

DETERMINATION OF PEAK DISCHARGE. The spike probability density function provided a better estimation of the time of occurrence of peak discharge than that obtained from an instantaneous frequency histogram, in which one interspike interval could incorrectly represent the peak in an envelope of neural activity. For most of the orienting gaze shifts that we analyzed, a single peak of oTR(S)N activity was easily discernible from the spike probability density function. On those few instances when there were two peaks of equal height in the cell's discharge profile, we chose the first peak as an estimation of the time of occurrence of peak discharge.

CORRELATION TO INSTANTANEOUS GAZE MOTOR ERROR. We also plotted the normalized spike probability density function against instantaneous gaze motor error (i.e., instantaneous vector amplitude between current and desired gaze positions). Zero degree gaze motor error indicated alignment of gaze on target. To produce these plots, we first aligned rasters of cell activity, obtained from between 3 and 10 movements of identical amplitude, on the end of the gaze shift. The average gaze, head, and eye trajectories were obtained. The averaged spike density function was then: *1*) calculated; *2*) normalized using the value of the cell's highest peak discharge obtained in all of the utilized trials covering the whole amplitude range; and *3*) delayed by 10 ms with respect to the occurrence of the averaged gaze shift. This time was chosen because it represented the average time between a burst of TR(S)N discharge and a reacceleration of the gaze trajectory (see Fig. 4, *B–D*, and Table 1). This also corresponded to the time to reacceleration of gaze when the SC was microstimulated during the execution of an orienting gaze shift (see Fig. 6 and Table 1).

RESULTS

We collected enough data from 75 TR(S)Ns to allow for a description of their movement-related discharge properties. These cells were located throughout the rostrocaudal extent of the SC in 10 cats. They were classified as either fixation (10/75) or orientation (65/75), on the basis of criteria established in the two preceding papers (Guitton and Munoz 1991; Munoz and Guitton 1991). We first describe the typical discharge patterns recorded from oTR(S)Ns when cats generated orienting movements in

different behavioral situations. Initially, we consider oTR(S)N discharges associated with gaze shifts, the directions and magnitudes of which match the optimal gaze position error vector for each cell. This vector corresponded to the gaze position relative to a target of interest that generated the greatest sustained discharge when the visual axis was stationary (Munoz and Guitton 1991). Then, we consider the pattern of activity across the entire SC as cats generated gaze shifts of various amplitudes along the optimal direction. It will be demonstrated that, during an orienting movement, as the visual axis is driven toward the target, the instantaneous location of TR(S)N activity on the SC motor map continuously changes.

Influence of task on movement-related discharges of oTR(S)Ns

QUALITATIVE RELATIONS. In a given behavioral condition, oTR(S)Ns typically increased their discharge rate when a cat generated a single-step gaze shift, the direction and magnitude of which matched the cell's optimal gaze position error vector. Figure 1, *A* and *B*, illustrates the responses of

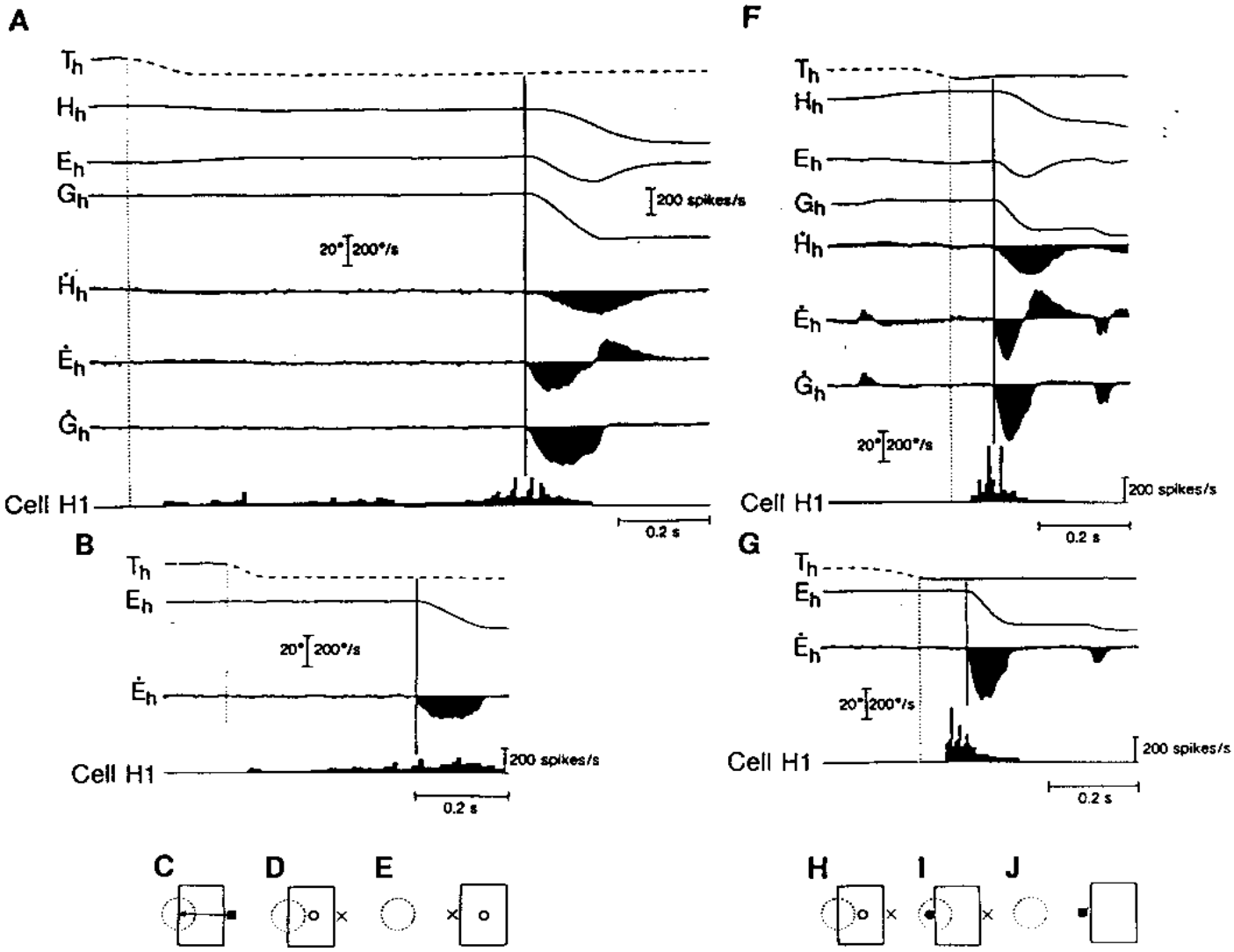

FIG. 1. Single examples of oTR(S)N discharge related to gaze shifts to predicted (*A* and *B*) and visible (*F* and *G*) targets with the head unrestrained (*A* and *F*) or fixed (*B* and *G*). *Top* to *bottom*: horizontal target (T_h), head (H_h), eye (E_h), and gaze (G_h) position traces; horizontal head ($\dot{H}_h$), eye ($\dot{E}_h$), and gaze ($\dot{G}_h$) velocity traces; and instantaneous frequency histogram of *cell H1* discharge. Vertical dashed lines mark time of target disappearance (*A* and *B*) or reappearance (*F* and *G*). Target trace is dashed whenever the target is hidden behind the barrier. Solid vertical lines mark onset of gaze shifts. *C–E*: schematic representations of the predicted-target condition. Briefly, the cat faced an opaque rectangular barrier depicted by the large rectangle. Cell was located in the caudal right SC and had its visual receptive field (dashed circle) situated on the horizontal meridian, to the left of the point of fixation (marked by X). Gaze position error field of an oTR(S)N was coextensive with its visual receptive field (Munoz and Guitton 1991). Therefore the vector drawn from the fixation point to the center of the dashed circle represents the cell's optimal gaze position error vector. Food target (filled circle) was initially visible on the right side of the barrier (Fig. 1*C*). Target was then hidden behind the barrier (Fig. 1*D*), and the trained animal oriented to the left side (Fig. 1*E*). *H–J*: schematic representations of the visible-target condition. Food target was initially hidden behind the barrier until the animal directed its visual axis to the right side (Fig. 1*H*). Target was then unexpectedly and rapidly moved to the left side, within the visual receptive field of *cell H1* (Fig. 1*I*), and the cat oriented leftward to the visible target (Fig. 1*J*).

an oTR(S)N, *cell H1*, when the cat oriented to the predicted target. A schematic representation of the experimental condition is provided in Fig. 1, *C–E*. The discharge pattern recorded from the oTR(S)N was similar when the animal oriented to the predicted target in the head-free (Fig. 1*A*) and head-fixed (Fig. 1*B*) conditions. The neuron, initially silent while the cat fixated the target to the right, began to discharge a low-frequency train of action potentials ~60–80 ms after the target disappeared. *Cell H1* continued to fire until the end of the leftward gaze shift, which eliminated this error. There was a modest increase in the firing rate of the neuron, which occurred immediately before movement onset and which was associated with the orienting response itself; it was clearly dissociated from the initial onset of sustained activity that followed target disappearance.

Figure 1, *F* and *G*, illustrates the activity of the same oTR(S)N when the cat oriented to the suddenly appearing

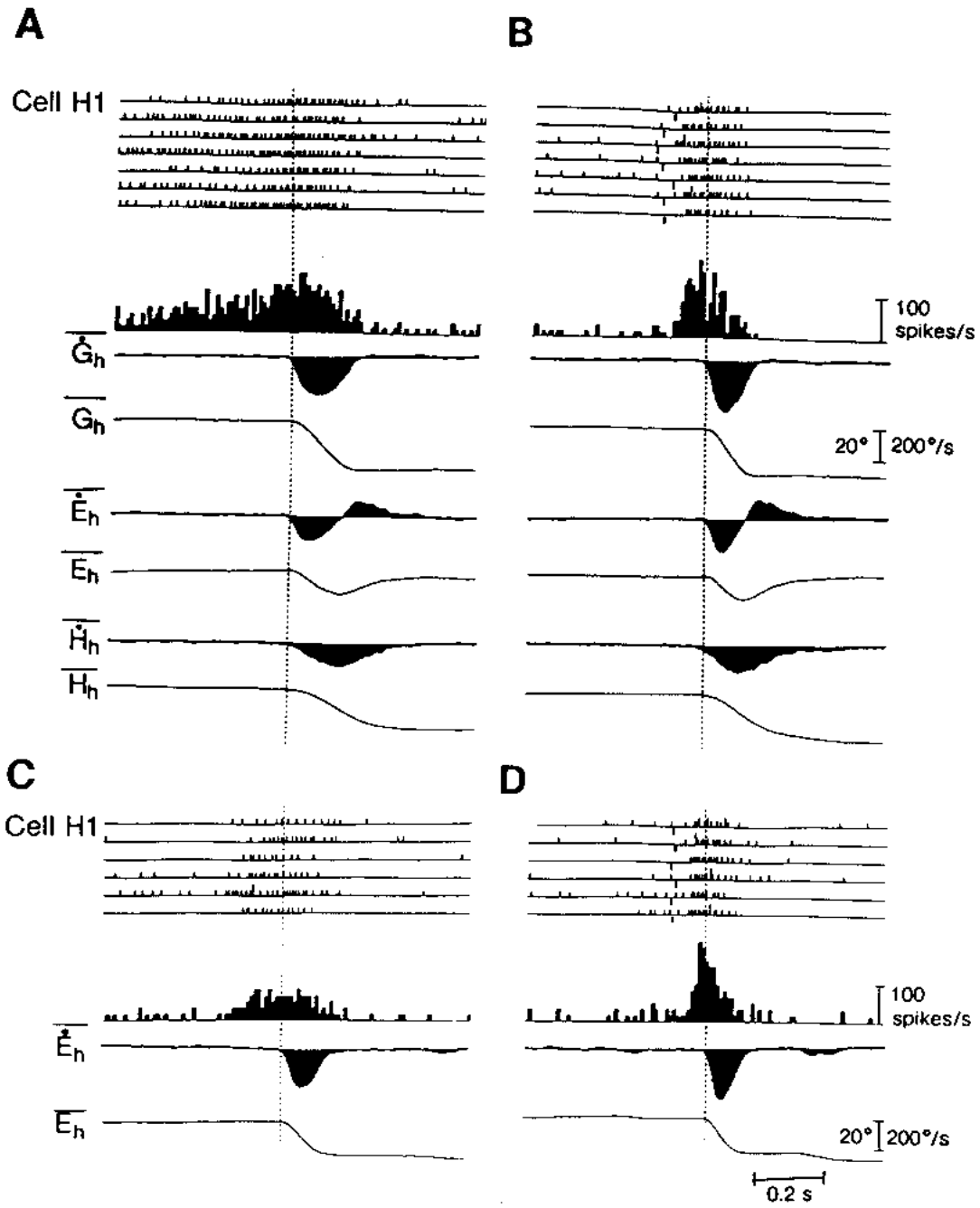

FIG. 2. Comparison of several examples of oTR(S)N discharge patterns related to movements to predicted (*A* and *C*) and visible (*B* and *D*) targets when the head was free (*A* and *B*) and fixed (*C* and *D*). In each section, from *top* to *bottom*; rasters of cell discharge; a summary histogram; and computer-averaged velocity and position traces for gaze, eye, and head. Traces are aligned on the onset of the gaze shifts (vertical dashed lines). Tick marks *beneath* each trace of unit discharge, in *B* and *D*, indicate when the target appeared. See legend of Fig. 1 for additional details. All movements closely matched the cell's gaze position error vector.

visible food target. The oTR(S)N had a similar discharge pattern irrespective of whether the head was free (Fig. 1*F*) or fixed (Fig. 1*G*). The neuron began to discharge a high-frequency burst of action potentials ~50 ms after the target appeared within its visual receptive field. This abrupt onset of neural activity preceded movement onset by ~50 ms. The cell ceased firing at the end of the gaze shift to the visible target. The high-frequency burst was consistently initiated some 50 ms after the sudden appearance of the target in the neuron's visual receptive field. The close temporal relationship between the burst of spikes and the onset of the orienting gaze shift suggested that this activity was also related to the execution of the movement.

Figure 2 compares several responses, recorded from the same oTR(S)N, associated with gaze shifts whose amplitudes and directions matched the optimal gaze position error vector for the cell. The panels show movements to the predicted and visible targets with the head free and fixed. The histograms in Fig. 2 all show an increase in neuronal activity, which immediately preceded movement onset. Note that both the movement-related firing pattern of the cell and the speed of the orienting movement were dependent on whether the cat was in the predictive or visible-target mode. Not only did the computer-averaged gaze, eye, and head velocity profiles all reach higher levels when the target of the orienting movement was visible, so too did the histogram of unit activity.

The discharge patterns recorded from most oTR(S)Ns were qualitatively similar to that of cell H1, as illustrated in Figs. 1 and 2. Ninety-five percent (62/65) of the oTR(S)Ns we studied increased their rate of discharge, beyond that of the sustained discharge, before visually triggered gaze shifts, the amplitudes and directions of which matched the cell's optimal gaze position error vector. Forty-six oTR(S)Ns were also tested in the predicted-target condition. Seventy-six percent of these cells (35/46) showed an increase in activity immediately before movement onset. The remaining 24% (11/46) of the neurons were tonically active before predictive gaze shifts but presented no phasic increase in discharge at movement onset (e.g., see Figs. 1 and 2 of Munoz and Guitton 1986). The intensity of the phasic neuronal response in the visible-target condition was, in general, higher than in the predicted-target condition. TR(S)N discharges related to spontaneous movements were not studied in detail because cats rarely generated spontaneous gaze shifts having a large range of amplitudes and directions. Nonetheless, some oTR(S)Ns were phasically active, albeit weakly, for some spontaneous movements made in the dark.

QUANTITATIVE RELATIONS BETWEEN DISCHARGE FREQUENCY AND MOVEMENT SPEED. Figure 3, *A–C*, shows the relation between average discharge rate (see METHODS) of cell H1 and the peak velocity of the eye, head, and gaze trajectories

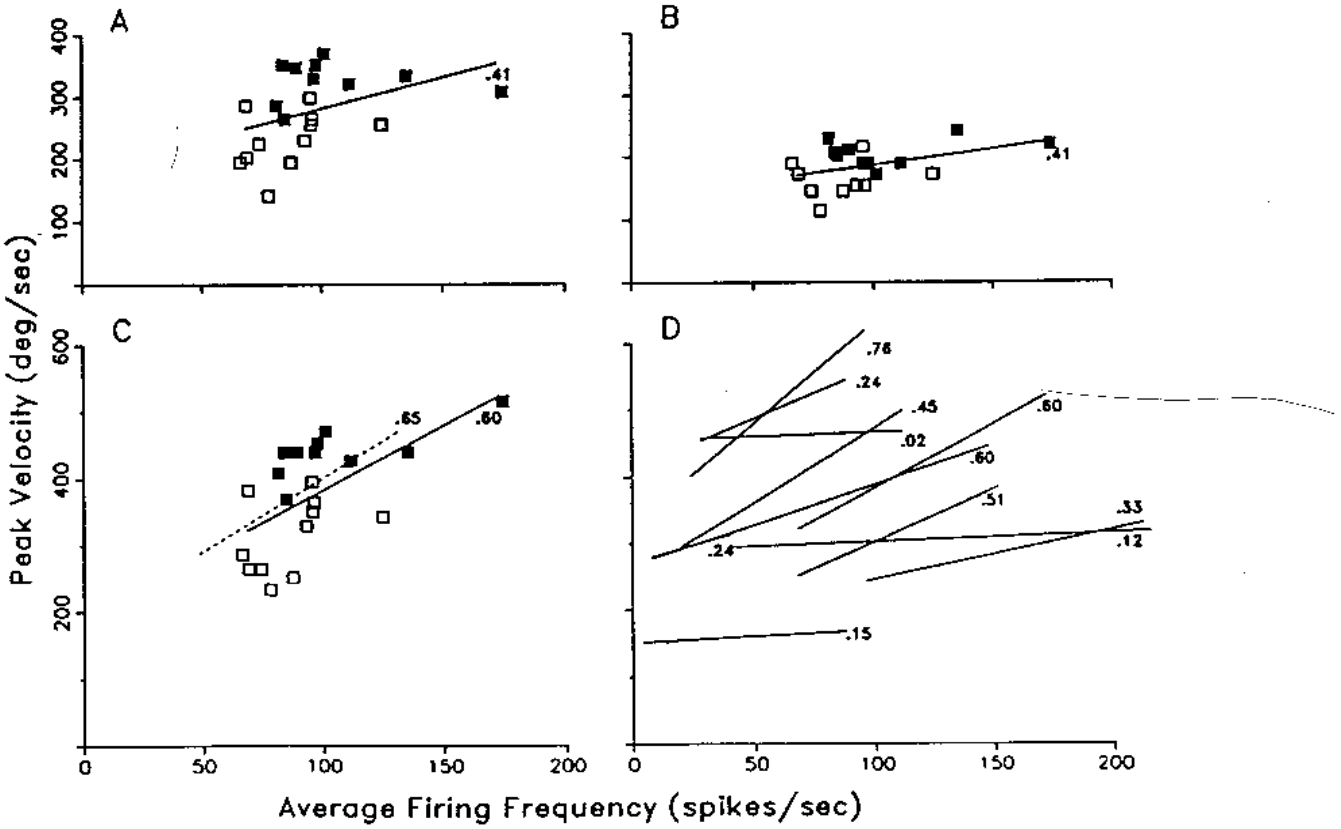

FIG. 3. Relationship between the average firing frequency of an oTR(S)N and peak eye (*A*), head (*B*), and gaze (*C*) velocity for head-free gaze shifts, the directions and amplitudes of which matched the cell's optimal gaze position error vector. Data points taken from movements to predicted (□) and visible (■) targets. Solid lines through the data are produced by a regression analysis of head-free data. Dashed line in *C* corresponds to similar analysis of head-fixed data (individual data points not shown). *D*: regression lines and correlation coefficients showing relationships between peak gaze velocity and average discharge frequency of 11 oTR(S)Ns for movements generated when the head was unrestrained.

for horizontal leftward gaze shifts that were 24–32° in amplitude. This vector of movement matched the cell's optimal gaze position error vector. The data were obtained from movements to both visible (■) and predicted (□) targets. Regression analyses generated the solid lines, with correlation coefficients presented to the *right* of each line. The slopes of the lines in Fig. 3, *A–C*, were all significantly different from zero (*t* test, $P < 0.05$). The dashed line in Fig. 3*C* was obtained from a regression analysis of similar data obtained when the cat's head was fixed ($r = 0.65$, $n = 19$). Note that the correlations between the discharge rate of the cell and peak eye (Fig. 3*A*) and head (Fig. 3*B*) velocities were weak, whereas the correlation to gaze (Fig. 3*C*) was stronger. This was the case for all cells analyzed.

Note that another study (Berthoz et al. 1986) found that TRSN burst profiles could be matched to saccadic eye velocity profiles when shifted by ~50 ms. We also calculated the average firing frequency of oTR(S)Ns using an interval spanning 50 ms before movement onset through 10 ms before its termination. This method yielded similar correlations between average firing frequency and movement velocity.

Figure 3*D* summarizes, for 11 oTR(S)Ns that we studied in detail, the regression analyses between average discharge rate and peak gaze velocity (head free) for movement vectors that matched each cell's optimal gaze position error vector. Correlation coefficients ranged from 0.02 to 0.76. All lines with coefficients >0.30 were significant (*t* test, $P < 0.05$). The cells that had discharge rates correlated to movement velocity were distributed across the SC motor map. We conclude from these analyses that at least some of the oTR(S)Ns influence the speed of an orienting response.

Sensory responses of oTR(S)Ns modulate ongoing movements

We now present evidence demonstrating how visually evoked changes in discharge frequency of oTR(S)Ns can have a direct "on-line" influence on the trajectories of eye, head, and gaze orienting movements. We consider orienting responses that were triggered using both predictive and visual cues. In this situation, the food target was moved from one side of the barrier to reappear on the other side, and the gaze shifts to reorient the visual axis onto the food occurred either before or after target reappearance. Examples of such head-free orienting movements are shown in Fig. 4 along with the associated neuronal activity of an oTR(S)N (cell H1). Each trial begins with the cat fixating the food target located on the right side of the barrier, thereby placing the left edge in the visual receptive field of the neuron. The target was then moved behind the barrier and reappeared on the left. The orienting movement was initiated either before (Fig. 4*A*) or after (Fig. 4, *B–E*) target reappearance. There was a continuum of response latencies between these two conditions (e.g., see Fig. 5 of Guitton et al. 1990). Each trial terminated with the cat fixating the target on the left.

In each of the trials illustrated in Fig. 4, the oTR(S)N began to discharge shortly after the target disappeared from the right side and continued to fire until the end of the leftward gaze shift. In Fig. 4*A*, the movement began before the target reappeared from behind the barrier and was therefore triggered by predictive cues. In association with these predictive movements, the neuron discharged a low-frequency train of action potentials. Furthermore, the gaze velocity profile appeared somewhat flat-topped or blunt, a characteristic of predictive gaze shifts (Guitton et al. 1990). In Fig. 4*E*, the orienting movement began >50 ms after the target reappeared; and the cell, in addition to carrying the low-frequency sustained discharge, also discharged a high-frequency burst of spikes that began ~40 ms after the target reappeared and ~25 ms before the onset of the gaze shift. In this condition the eye, head, and gaze velocity profiles had greater accelerations and reached higher velocities than the profiles of movements triggered in the absence of the oTR(S)N burst (Fig. 4*A*). We have previously reported that, in the barrier paradigm, gaze shifts that began >50 ms

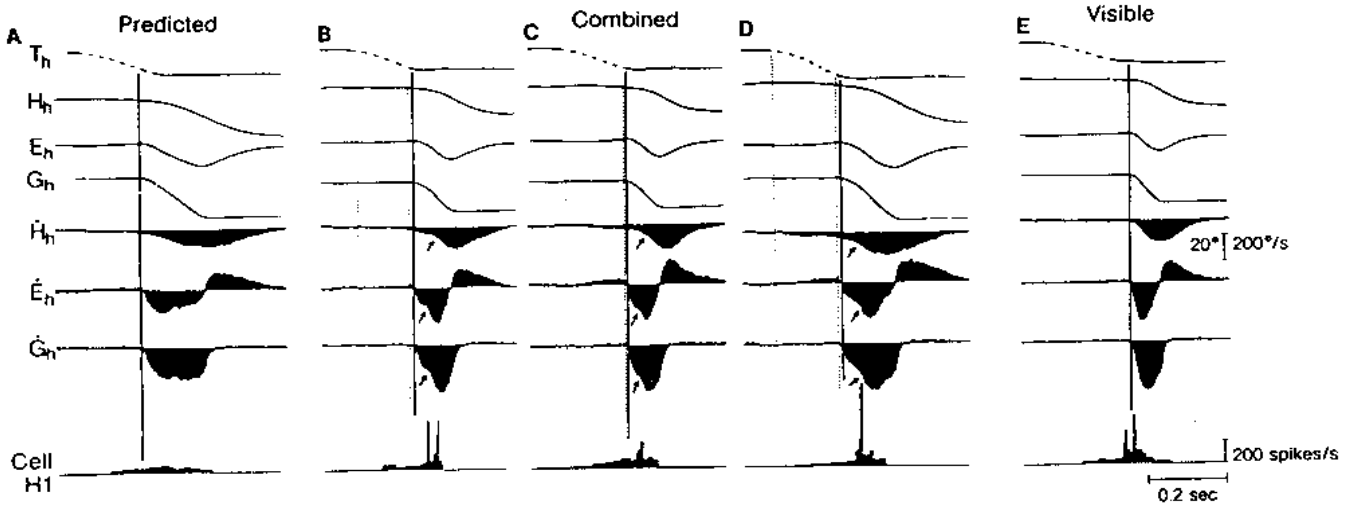

FIG. 4. Combined effects of prediction and vision on the discharge of an oTR(S)N and the trajectory of combined eye-head orienting movements. Food target was moved from the right to the left side of the barrier and the cat oriented either before (*A*) or after (*B–E*) target reappearance. Symbols as in Fig. 1. Left and right vertical dashed lines mark target disappearance and reappearance, respectively. Solid vertical line denotes onset of the gaze shifts.

after the target reappeared all had similar, sharply pointed velocity profiles and were considered to be visually triggered (Guitton et al. 1990).

Gaze shifts triggered within 0–50 ms after the target reappeared belonged to a transition zone between movements that were either predictively or visually triggered. Examples of head-free gaze shifts, triggered within this transition zone, are illustrated in Fig. 4, *B–D*. After the initial increase in velocity, there existed in each of the eye, head, and gaze traces a deceleration phase, which suggested that peak velocity was soon to be attained. The velocity at each arrow is comparable with the peak velocity in the adjacent traces of Fig. 4*A*, thereby suggesting that the eyes, head, and therefore gaze in Fig. 4, *B–D*, were driven, at least initially, by discharges characteristic of movements to predicted targets. However, as evidenced by the inflection point on each trace (marked by ↗) the trajectory of the orienting response was modified in midflight; all profiles showed a reacceleration, thereby assuming a new shape that was more characteristic of a gaze shift to a visible target. Note that the discharge pattern of the oTR(S)N showed changes that were comparable with the modified movement trajectories. At the onset of the gaze shift, the cell was firing at only a low-frequency rate, a pattern of activity characteristic of movements to the predicted target. Shortly after target reappearance, but within the gaze shift, the neuron discharged a high-frequency burst of spikes. This increase in firing frequency, which followed target reappearance by ~40–50 ms, was visually evoked, yet also appeared to be motor-related because it preceded the modification in the eye, head, and gaze trajectories. The abrupt increase in cell discharge drove the instantaneous firing frequency profile from a low (i.e., <100 Hz) to a high level. The first interspike interval <10 ms (i.e., >100 Hz) preceded the reacceleration of gaze and eye by 9 ± 1 (SD) ms (n = 7) and of the head by 29 ± 2 (SD) ms (n = 7). Table 1 summarizes similar data obtained from six TR(S)Ns recorded in two different cats. Note that the latency from burst onset to movement reacceleration was very similar for all six cells. The latency from the abrupt increase in oTR(S)N firing rate to the reacceleration of the gaze and eye trajectories ranged from 8 to 12 ms, with a population average of 10 ms. The latencies to head reacceleration were considerably longer, ranging from 24 to 34 ms, with a mean of 29 ms. However, because the head has a greater biomechanical lag, the same signal appeared to produce reacceleration of both the eye and head trajectories.

Microstimulation of the SC

The data presented in Fig. 4 and Table 1 suggested that the intensity of oTR(S)N discharges may specify some of the temporal characteristics of an orienting movement (i.e., latency and velocity). To further investigate this influence, we tested whether electrical stimulation mimicking TR(S)N discharge could produce similar behavioral effects. We compared the trajectories of movements that were elicited with different patterns of electrical microstimulation applied to the SC at the site of identified oTR(S)Ns.

STIMULATION FREQUENCY INFLUENCES MOVEMENT LATENCY AND VELOCITY. Figure 5 illustrates how the frequency of a train of stimulus pulses influenced the latency and velocity

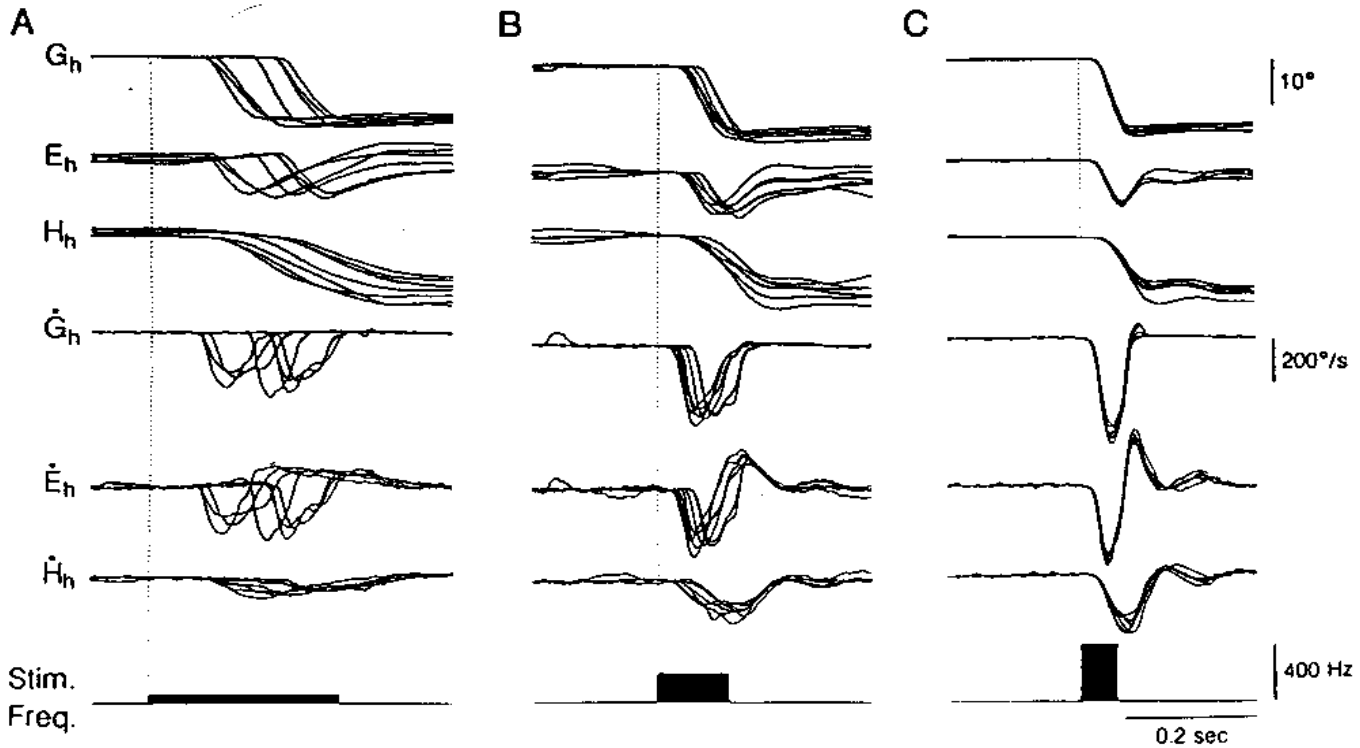

FIG. 5. Effects of varying stimulation frequency on trajectory of gaze shifts elicited by collicular microstimulation when the head was unrestrained. Stimulation train consisted of 20 stimulus pulses at 75 (*A*), 200 (*B*), or 400 Hz (*C*). Duration and frequency of stimulation are represented by the *bottom trace*. Symbols as in Fig. 1.

TABLE 2. *Effect of frequency of collicular microstimulation on elicited movements*

Cat	Component	Frequency, Hz	n	Amplitude, deg	Velocity, deg/s	Latency, ms
J	Gaze	66	6	11.2 ± 2.4	189 ± 18*	129 ± 43*
		333	8	12.6 ± 1.4	382 ± 38	25 ± 1
	Eye	66	6	8.2 ± 2.1	164 ± 21*	130 ± 44*
		333	8	8.5 ± 1.1	325 ± 42	25 ± 1
	Head	66	6	6.5 ± 1.9	55 ± 10*	102 ± 32*
		333	8	7.0 ± 1.8	141 ± 31	39 ± 5
S	Gaze	75	18	12.5 ± 1.5†	212 ± 35†	131 ± 52†
		200	20	14.3 ± 1.9	326 ± 37	33 ± 11
		400	12	15.3 ± 0.9	435 ± 24‡	19 ± 2‡
	Eye	75	18	8.9 ± 1.0	182 ± 27†	132 ± 52†
		200	20	9.0 ± 1.2	254 ± 33	33 ± 11
		400	12	9.8 ± 0.7	334 ± 28‡	19 ± 2‡
	Head	75	18	10.2 ± 1.5	70 ± 12†	125 ± 32†
		200	20	11.1 ± 2.2	145 ± 25	40 ± 10
		400	12	9.8 ± 1.3	218 ± 27‡	31 ± 3‡

Values are means ± SD; n, number of observations. Significant difference (t test, $P < 0.01$) *between 66 and 333 Hz stimulation, †between 75 and 200 Hz stimulation, and ‡between 200 and 400 Hz stimulation.

of the evoked movements. Stimulation was delivered when the cat looked straight ahead at a blank barrier with no food target present. Increasing the frequency led to covariant increases in the velocity of the eye, head, and gaze movements and to shorter, less variable latencies from stimulation onset to movement onset. These observations, obtained from two cats, are summarized in Table 2. There was little or no difference in the amplitudes of the elicited movements, but the differences in movement velocity and latency were highly significant. The positive effect of stimulation frequency on movement velocity resembles the relationship between the average firing frequency of at least some oTR(S)Ns and the peak velocity of eye, head, and gaze trajectories during natural movements (see Fig. 3).

MOVEMENT REACCELERATION AFTER A BURST OF COLLICULAR STIMULATION. In a second stimulation experiment, we studied the effect of a short train of stimulation (2–4 pulses at 500 Hz) delivered during a natural, head-free gaze shift which mimicked the on-line TR(S)N bursts that preceded reacceleration of eye, head, and gaze trajectories (Fig. 4). Stimulation was applied to the collicular locus that was active at the start of the natural gaze shift. The brief high-frequency train was presented before, during, and after predictively triggered gaze shifts. This brief burst of stimulation did not initiate any motion of the eyes or head when it was presented either before movement onset or after movement termination. However, when presented during the gaze shift, the trajectory of the ongoing movement was modified. Shown in Fig. 6*A* is a control response (——) and a test response (– – –) during which a four-pulse train of electrical stimulation was applied to the caudal right SC during the leftward movement. The onset of stimulation is denoted by the vertical dotted line. Both the eye and head trajectories, and consequently the gaze trajectory, were reaccelerated in midflight by the sudden presentation of the high-frequency stimulation. The mean latency from onset of the stimulation to reacceleration of the eye, head, and gaze trajectories is summarized for two cats in Table 1. The eye and gaze trajectories reaccelerated after 10–11 ms, whereas the head trajectory was modified 23–24 ms after stimulation onset. These latencies are similar to those obtained after the onset of an oTR(S)N burst occurring during a gaze shift (Fig. 4 and Table 1). Furthermore, note that the latency from the onset of stimulation to movement reacceleration was shorter than that from the onset of stimulation trains to the initiation of movement when the visual axis was stationary at stimulation onset (compare latencies in Tables 1 and 2).

The latency to movement reacceleration that followed the brief high-frequency train depended on when in the time course of the natural movement the stimulation was applied. Figure 6*B* explores this point in greater detail. A low-frequency (66 Hz), long-duration (260 ms) train of stimulation preceded a high-frequency (333 Hz), short-duration (40 ms) train. This pattern roughly mimicked the discharges of oTR(S)Ns that were recorded when the cat oriented to the visible food target after presentation of both predictive and visual cues (see Fig. 4, *B–E*). Stimulation intensity was set at 40 μA, which was twice the threshold current required to elicit a movement from this collicular site when a train of 300 Hz was used. The *top 11 traces* show the eye velocity profiles obtained from single trials when the head was fixed. The trials are rank ordered on latency to the first saccade, the latency of which was extremely variable when initiated by the low-frequency train (see Table 2). The *bottom trace* represents the instantaneous stimulation frequency. The low-frequency train began ~100 ms before the start of the traces in Fig. 6*B*.

The presence of the low-frequency "preamble" of stimulation had a dramatic effect on the latency of movements elicited by the high-frequency burst. When the high-frequency stimulation was presented alone in the head-fixed condition, without the low-frequency train, saccades were elicited after a mean latency of 21 ± 3 (SD) ms (n = 23), as marked by the arrow under the velocity traces. The *top two traces* in Fig. 6*B* show trials in which the low-frequency stimulation failed to evoke a saccade and movement was initiated only after the high-frequency stimulation began. The vertical dashed line denotes onset of these movements. The mean latency to saccade onset in trials of this type was 13 ± 2 (SD) ms (n = 15), which was significantly less than

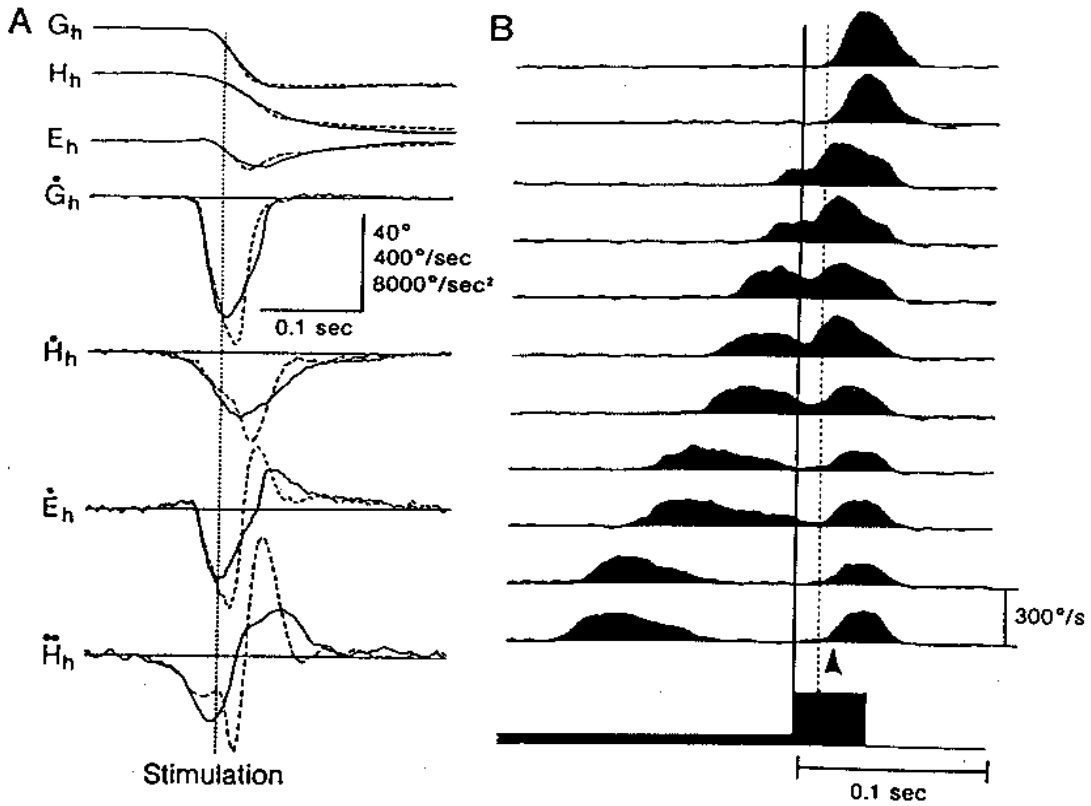

FIG. 6. *A*: superimposition of single leftward gaze shifts to the predicted target, either when a brief burst of stimulation was delivered to the caudal right SC at the time indicated by the vertical dotted line (- - -) or when no stimulation occurred (——). $\ddot{H}_h$, head acceleration. Other symbols as in Fig. 1. Note that the stimulation produced a short-latency reacceleration in movement trajectory. *B*: instantaneous eye velocity profiles from 11 trials when low (66 Hz)- and high (333 Hz)-frequency trains were presented sequentially in the head-fixed condition. Vertical solid line marks the onset of the high-frequency train of stimulation. Vertical dashed line marks latency to saccades in *top 2 traces*. Arrow indicates onset time of saccades evoked when the high-frequency train of stimulation was used alone, without the low-frequency preamble.

movements initiated by the high-frequency train alone [$t(14) = 6.74$, $P < 0.0005$]. The bottom *four velocity profiles* in Fig. 6*B* represent trials for which the low-frequency stimulation triggered a saccade that terminated just before onset of the high-frequency train. In this condition, the mean latency to onset of the saccade elicited by the high-frequency burst was 15 ± 2 (SD) ms ($n = 10$), which also was significantly less than movements initiated by the high-frequency train alone [$t(9) = 6.47$, $P < 0.0005$] but not significantly different from the latency obtained when only one saccade was evoked, as in the *top two traces* [$t(9) = 2.45$, $P > 0.01$].

The *third to seventh traces from the top* in Fig. 6*B* illustrate a third response type, in which low-frequency stimulation triggered a saccade that was ongoing when the high-frequency train began. The saccades, although in midflight, reaccelerated shortly after onset of the high-frequency train. Note that the time to reacceleration generally preceded the vertical dashed line. The average latency from onset of the high-frequency train to reacceleration of the eye in these trials was quite variable (11 ± 4 ms, mean ± SD; $n = 8$); its average value is similar to the latency to gaze reacceleration after oTR(S)N bursts (see Table 1).

Movement fields of oTR(S)Ns

We now consider the movement fields of oTR(S)Ns and show that they do not have the classically defined, circumscribed movement fields reported for monkey saccade-related burst cells (Mohler and Wurtz 1976; Schiller and Koerner 1971; Sparks et al. 1976; Wurtz and Goldberg 1971, 1972a). The data described in this section were obtained from recording oTR(S)N movement-related phasic responses when head-free cats generated predictively triggered gaze shifts of various amplitudes and directions.

Figures 7 and 8 illustrate activity recorded from two oTR(S)Ns (*cells Q24* and *Q37*, respectively) as a cat generated single-step gaze saccades of different amplitudes in the direction of each cell's optimal gaze position error vector. The traces are aligned on onset (Figs. 7, *A–D* and 8, *A–D*) and termination (Figs. 7, *E–H* and 8, *E–H*) of the gaze saccades. The optimal gaze position error vectors of the cells were 15° horizontal-right (*cell Q24*) and 55° down-left at an angle of 45° to the horizontal (*cell Q37*). Their sensitivity to gaze shift amplitude is our focus here. Cell Q24 was located, stereotaxically, ~1.5 mm rostral to *Q37*. Microstimulation at the sites of *Q24* and Q37 elicited gaze shifts that were, respectively, 13 and 70° in magnitude.

Cell Q24 discharged in relation to all horizontal rightward gaze shifts that were larger than ~5° in amplitude (Fig. 7). However, the timing of occurrence of peak discharge (marked by arrows in Fig. 7) depended on the amplitude of the movement. For 10 and 15° gaze shifts, peak discharge occurred synchronously with and shortly after, respectively, the start of the movements (Fig. 7, *A* and *B*).

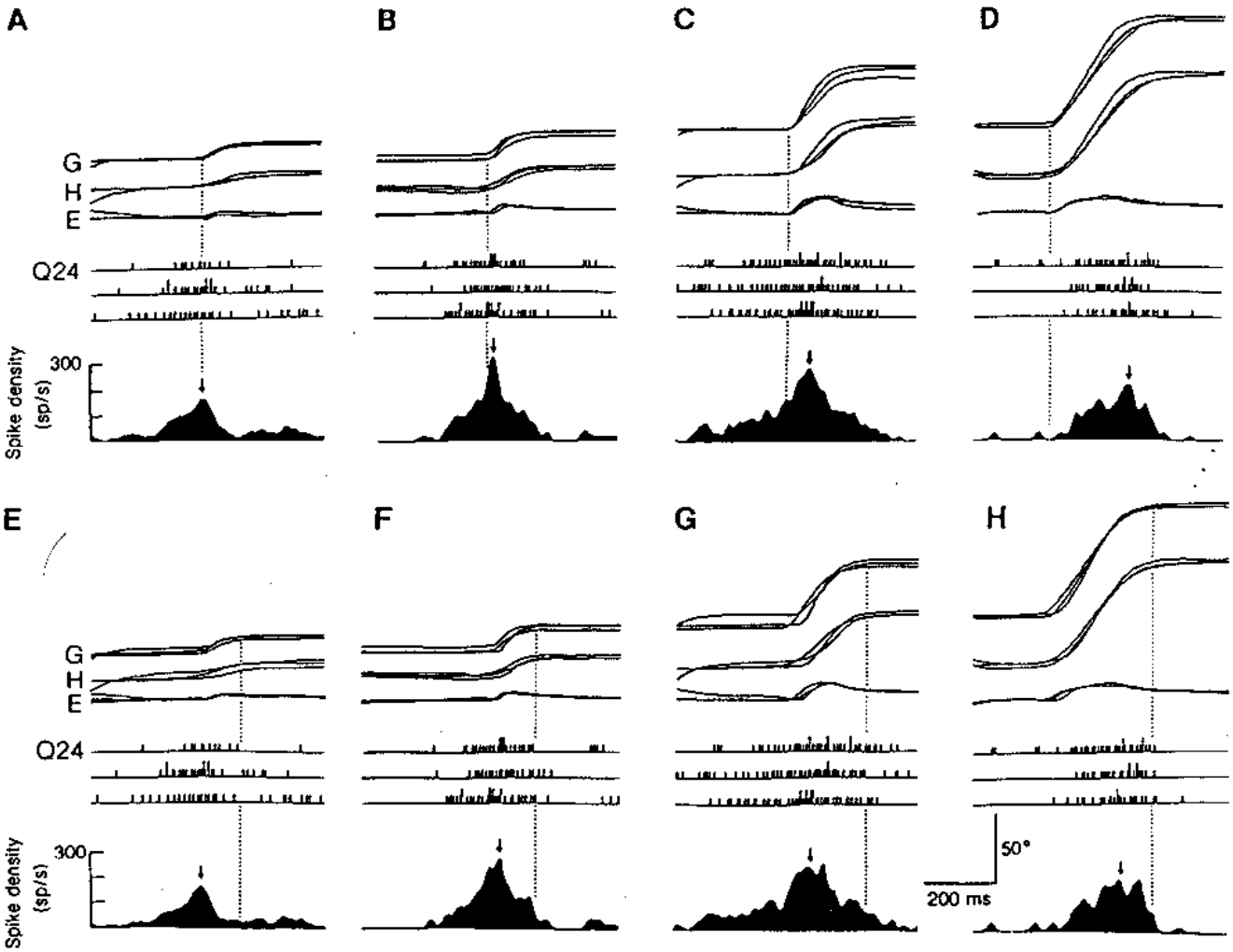

FIG. 7. Movement-related discharges of an oTR(S)N (*cell Q24*, the optimal gaze position error vector of which was 15° in magnitude) for predictively triggered gaze shifts of different amplitudes along the optimal direction. Traces are aligned (vertical dotted lines) on the onset (*A–D*) and termination (*E–H*) of gaze shifts. *Top* to *bottom* in each panel: gaze (G), head (H), and eye (E) position traces; neural discharge of *cell Q24* (3 trials); and the spike density function (number of action potentials/second; see METHODS). Vertical arrows point to the peak discharge. In the *middle 3 traces*, the occurrence of an action potential, or spike, is represented by a small vertical line. Additional small lines superimposed on top of others indicate extra spikes within the same 2-ms time bin.

For 80° gaze shifts (Fig. 7*D*), the cell was silent at movement onset (i.e., no premovement sustained discharge) and peak discharge was attained late in the gaze shift. For 40° movements (Fig. 7*C*), the cell's discharge peaked closer to movement onset than in Fig. 7*D* but further than in Fig. 7*B*. Because the occurrence of peak discharge occurred later and later with respect to the onset of larger and larger movements (Fig. 7, *A–D*), the occurrence of the peak relative to the end of the movement (Fig. 7, *E–H*) remained somewhat constant and independent of movement amplitude. The above observations are inconsistent with the descriptions of the classic movement fields of vector-tuned neurons in the monkey SC; we shall elaborate on these points later.

Cell Q37 was located more caudally than Q24 and thus should be involved in initiating larger amplitude gaze shifts. Indeed, Q37 was most active before the 50 and 70° gaze shifts (Fig. 8, *C* and *D*), had a weaker discharge before the 25° movements (Fig. 8*B*), and gave only a few spikes before the 10° movement (Fig. 8*A*). Note the large range of gaze shift amplitudes over which the discharge of Q37 preceded movement onset. This is characteristic of cells in the caudal SC and is correlated with the nonlinear characteristics of the retinotopic motor map: in the caudal SC, a small zone of the motor map represents a wide range of amplitudes. We could not test Q37 for amplitudes >70° because the animal did not generate such large oblique movements in a single step. Because the peak discharge of Q37 always occurred immediately before movement onset (Fig. 8, *A–D*), the latency from the end of the movement to the peak increased for larger and larger movements as their durations increased (Fig. 8, *E–H*).

NUMBER OF SPIKES VERSUS MOVEMENT AMPLITUDE. The movement fields of cells Q24 and Q37 are analyzed quantitatively in Figs. 9, *A–C*, and 10, *A–C*, respectively. For simplicity, we plot only data obtained from gaze shifts along the optimal direction. (A cell's movement response became weaker as the difference between optimal and ac-

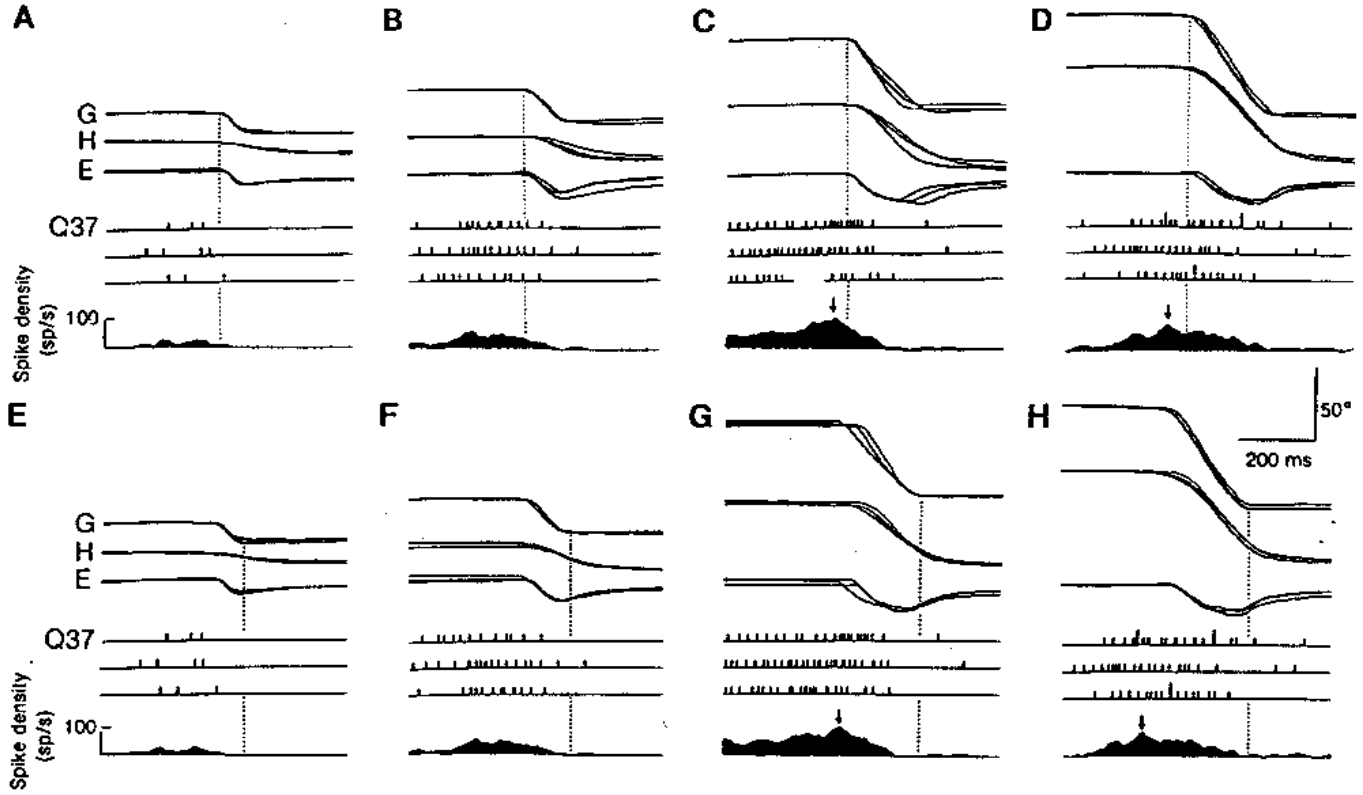

FIG. 8. Movement-related discharges of an oTR(S)N (*cell Q37*, the optimal gaze position error vector of which was >50° in magnitude) for predictively triggered gaze shifts of different amplitudes along the optimal direction. Traces are aligned (vertical dotted lines) on the onset (*A–D*) and termination (*E–H*) of gaze shifts. See legend to Fig. 7 for details.

tual movement directions increased.) The arrowheads *beneath* the abscissa in Figs. 9*A* and 10*A* mark the magnitude of each cell's optimal gaze position error vector (Munoz and Guitton 1991). Fewer spikes in the burst were counted as movement amplitude became progressively smaller than this optimal value. Both cells were phasically active for gaze shifts with magnitudes greater than the cell's optimal gaze position error vector. This was especially striking for cell Q24. As seen in Fig. 7*D*, this neuron was phasically active during 80° single-step gaze shifts but presented no premovement sustained discharge. All 15 oTR(S)Ns analyzed were found to behave in a similar fashion. The distal portions of their movement fields were open ended: the cells were active for all gaze shifts with directions that matched the cell's optimal gaze position error vector and with amplitudes that were equal to or greater than the magnitude of this vector.

We also plotted the number of spikes versus the amplitude of the eye and head components of the head-free gaze shift (Figs. 9, *B* and *C*, and 10, *B* and *C*). These eye and head movement fields were also open ended. The question of whether the oTR(S)N burst correlates best with gaze, head, or eye will be considered in a subsequent section.

TEMPORAL RELATIONS BETWEEN PEAK DISCHARGE AND ONSET AND TERMINATION OF ORIENTING MOVEMENTS. Although an oTR(S)N was active for all gaze shifts of an amplitude greater than its optimal gaze position error vector, we have seen in relation to Figs. 7 and 8 that the *timing* of the burst in the trajectory was dependent on the gaze shift amplitude. To illustrate this quantitatively, we measured the latency to peak discharge from onset and termination of each of the eye, head, and gaze trajectories and plotted these latencies against the total amplitude of each movement. In Figs. 9, *D–I*, and 10, *D–I*, we present these data obtained from cells Q24 and Q37, respectively. The solid lines in each plot were obtained by a linear regression analysis of the data. For cell Q24, the latency from the end of each gaze and head movement to peak discharge remained constant (Fig. 9, *G* and *I*) but increased for the eye movement component (Fig. 9*H*). For very large gaze shifts (e.g., Fig. 7*D*), peak discharge for cell Q24 frequently occurred after the eye reached its maximum deviation (i.e., points lying *above* the dotted line in Fig. 9*H*). From these observations it follows that the latency from movement onset to peak discharge for Q24 increased (Fig. 9, *D–F*), because the duration of gaze, eye, and head movements normally increases with amplitude (Guitton et al. 1990).

By comparison with cell Q24, as total gaze displacement increased, the latency from onset of the gaze, eye, and head movement components to peak discharge remained constant for cell Q37 (Fig. 10, *D–F*). Note the absence of data points in the low-amplitude range for cell Q37, corresponding to a lack of discharge in relation to small movements. We presume that cell Q37, unlike cell Q24, did not attain peak discharge after movement onset of large gaze shifts (almost no positive latencies in Fig. 10*D*) simply because the available gaze shifts were not large enough for this effect to be measurable (the magnitude of Q37's optimal gaze position error vector was ~55° in an oblique direction). As expected from the data in Fig. 10, *D–F*, the latency from the end of the eye, head, and gaze trajectories to peak dis-

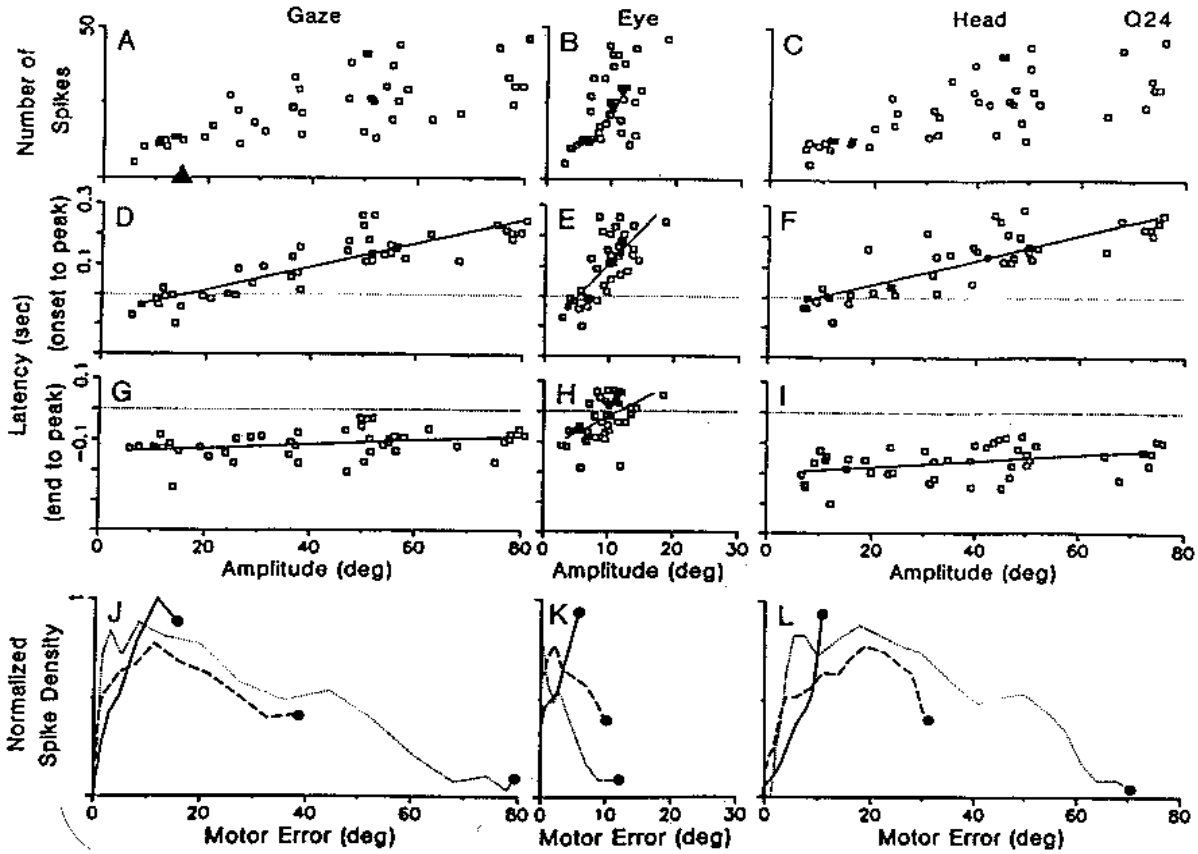

FIG. 9. Quantitative analysis of the burst discharges of oTR(S)N, *cell Q24*. Examples of this cell's discharge were presented in Fig. 7. Discharge parameters are compared with aspects of gaze, eye, and head trajectories in the predicted-target condition with the head unrestrained. *A–C*: plots of number of spikes vs. overall movement amplitude. *D–I*: plots of latency from movement onset (*D–F*) or termination (*G–I*) to peak discharge vs. overall movement amplitude. In *D–F*, positive latency means movement onset precedes peak discharge. In *G–I*, negative latency means peak discharge precedes movement end. Correlation coefficients for linear regression (——) lines are *D*, 0.88; *E*, 0.75; *F*, 0.83; *G*, 0.33; *H*, 0.54; and *I*, 0.39. *J–L*: plots of normalized spike probability density function (see METHODS) vs. instantaneous motor error. Gaze shifts begin at black dots and time runs toward zero motor error.

charge of cell Q37 decreased (i.e., became more negative) as movement amplitude increased (Fig. 10, *G–I*). As an aside, note that in association with large-amplitude, obliquely directed movements, the eye often started from an eccentric position in the orbit, accounting for eye amplitudes of up to 30° in the head-free condition. Comparable amplitude eye movements were absent from the Q24 data pool because the eye seldom went beyond 20° in the orbit during horizontally directed movements.

Figure 11 shows the plots of the latency from onset of the gaze shift to peak discharge for four more oTR(S)Ns recorded when the head was unrestrained. We were able to record cell activity related to gaze shifts with amplitudes well beyond the optimal gaze position error for the cells in Fig. 11, *A–C*. For each of these cells, the latency from onset of the movement to peak discharge increased for gaze amplitudes greater than the optimal error vector (represented by the filled triangles on the abscissas). The cell illustrated in Fig. 11*D* preferred very large gaze position errors (beyond 70°), and therefore we were unable to obtain data for single-step movements beyond the optimal. Results similar to those illustrated for the 6 oTR(S)Ns in Figs. 9, *D–I*, 10, *D–I*, and 11 were obtained from the other 10 cells we analyzed.

RELATIONS BETWEEN PEAK DISCHARGE AND INSTANTANEOUS MOTOR ERROR. To further investigate the mechanisms that determine when a phasic burst occurs, we compared the normalized spike density profiles of oTR(S)Ns with instantaneous gaze, eye, and head motor error for different amplitude movements (see METHODS). Figures 9, *J–L*, and 10, *J–L*, illustrate the curves obtained for cells Q24 and Q37, respectively. Time runs from right to left in these plots (i.e., toward 0° motor error). When plotted against gaze motor error (Figs. 9*J* and 10*J*), the spike density functions tended to assume the same trajectory, irrespective of the total gaze displacement. This was especially striking for cell Q24 (Fig. 9*J*). For 15° gaze shifts (——), cell Q24 attained peak discharge shortly after onset of the gaze saccade, when instantaneous gaze motor error was ~13°C. Neural activity then dropped toward zero as the gaze shifts were completed. For 80° gaze shifts (· · · ·), cell Q24 was initially almost silent. Neural activity built up during the movement, reached a peak at ~10° instantaneous gaze motor error, and then diminished as the gaze shifts terminated. A similar trajectory was also observed for 40° gaze shifts (– – –); peak activity was attained at ~12° instantaneous gaze motor error. For cell Q37, peak activity was achieved when instantaneous gaze motor error was ≥50° (Fig. 10*J*).

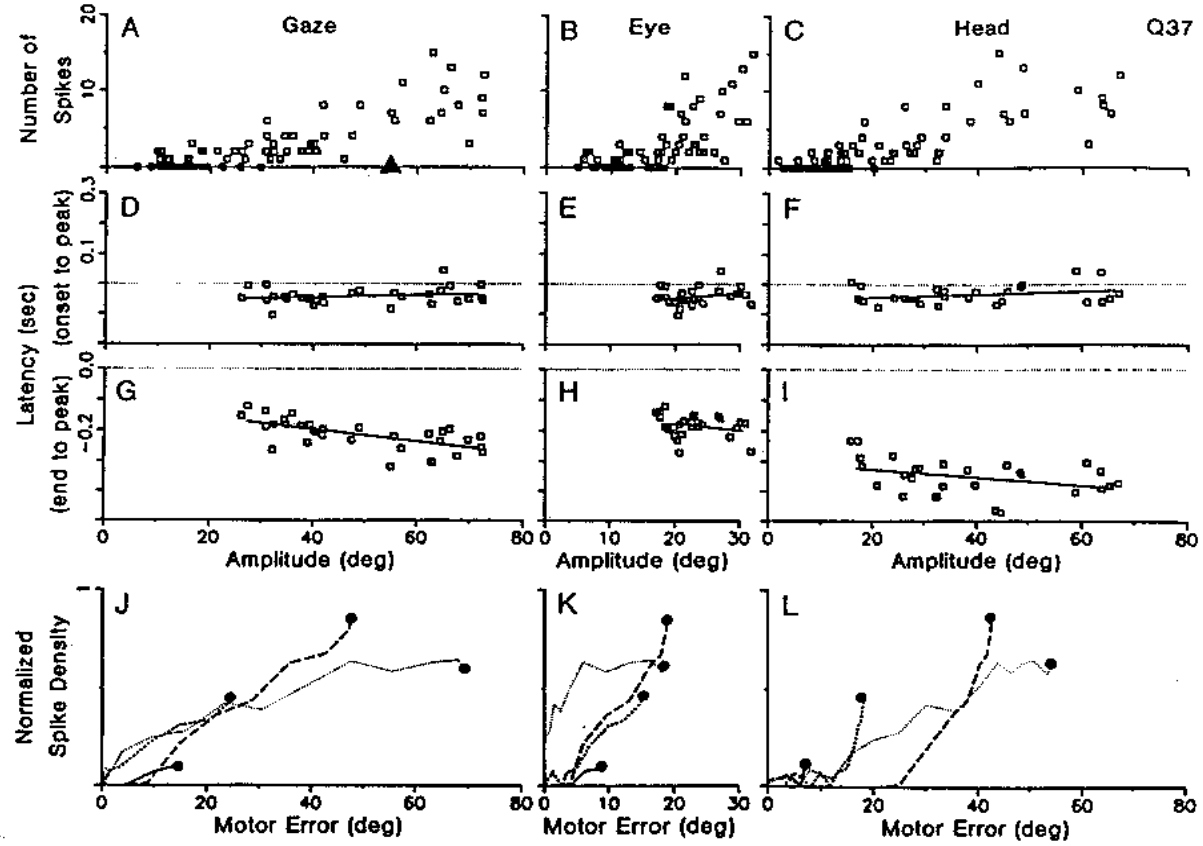

FIG. 10. Quantitative analysis of the burst discharges of oTR(S)N, *cell Q37*. Examples of this cell's discharge were presented in Fig. 8. Discharge parameters are compared with aspects of gaze, eye, and head trajectories in the predicted target condition with the head unrestrained. *A–C*: plots of number of spikes vs. overall movement amplitude. *D–I*: plots of latency from movement onset (*D–F*) or termination (*G–I*) to peak discharge vs. overall movement amplitude. Correlation coefficients for linear regression (——) lines are *D*, 0.20; *E*, 0.22; *F*, 0.24; *G*, −0.64; *H*, −0.24; and *I*, −0.37. *J–L*: plots of normalized spike probability density function vs. instantaneous motor error. Gaze shifts begin at black dots and time runs toward zero motor error. See legend to Fig. 9 for other details.

As gaze motor error diminished below this value, neural activity was also reduced. Thus each cell achieved its peak discharge in relation to a specific value of instantaneous gaze motor error.

The normalized spike density functions of oTR(S)Ns were also plotted against instantaneous eye motor error (Figs. 9*K* and 10*K*). We calculated eye motor error with respect to the maximum eye position in the trajectory of the eye relative to the head. For cell Q37, neural activity diminished as eye motor error was driven toward 0° for all amplitude gaze shifts (Fig. 10*K*). Note, however, that a very different picture emerged for cell Q24 (Fig. 9*K*). This cell's peak discharge preceded the onset of the eye saccade for small amplitude gaze shifts (Fig. 7*A*) but occurred during the plateau phase that follows the eye saccade (Guitton et al. 1984; Guitton and Volle 1987) for large-amplitude gaze shifts (Fig. 7*H*). Neural activity decreased with decreasing eye motor error for small movements (—— in Fig. 9*K*) but increased with decreasing eye motor error for large gaze shifts (· · · · in Fig. 9*K*). Thus, unlike for gaze motor error, the response of cell Q24 was clearly not modulated by eye motor error in the same way.

We also compared the normalized spike density functions of oTR(S)Ns to instantaneous head motor error (Figs. 9*L* and 10*L*). Both cells, Q24 and Q37, achieved peak discharge for some constant value of head motor error, in a manner similar to the relations to gaze motor error. This will be considered in more detail below.

Phasic movement-related discharges of oTR(S)Ns are best correlated to gaze motion

The results in the preceding sections suggested that each oTR(S)N reached its peak movement-related discharge when the visual axis was at a specific vector distance from the gaze position required to fixate the target. To demonstrate that oTR(S)N discharge was better related to gaze motor error than to head motor error, we compared data collected in head-fixed and head-free conditions.

Figure 12, *A* and *B*, contrasts the head-fixed (□) and head-free (■) gaze movement fields for two typical oTR(S)Ns. The magnitude of each cell's optimal gaze position error vector is denoted by the filled triangles on the abscissas. The spike count increased with gaze amplitude for both cells. We did not encounter cells with a distal border to their movement fields in either the head-fixed or head-free conditions. The range of amplitudes sampled in the head-fixed condition was restricted to ~30° by the limits in feline ocular motility. Nevertheless, the overlap in the data points in Fig. 12, *A* and *B*, suggests that gaze is the critical variable to which the phasic burst is correlated.

This is further tested in Fig. 12, *C* and *D*, where we plot

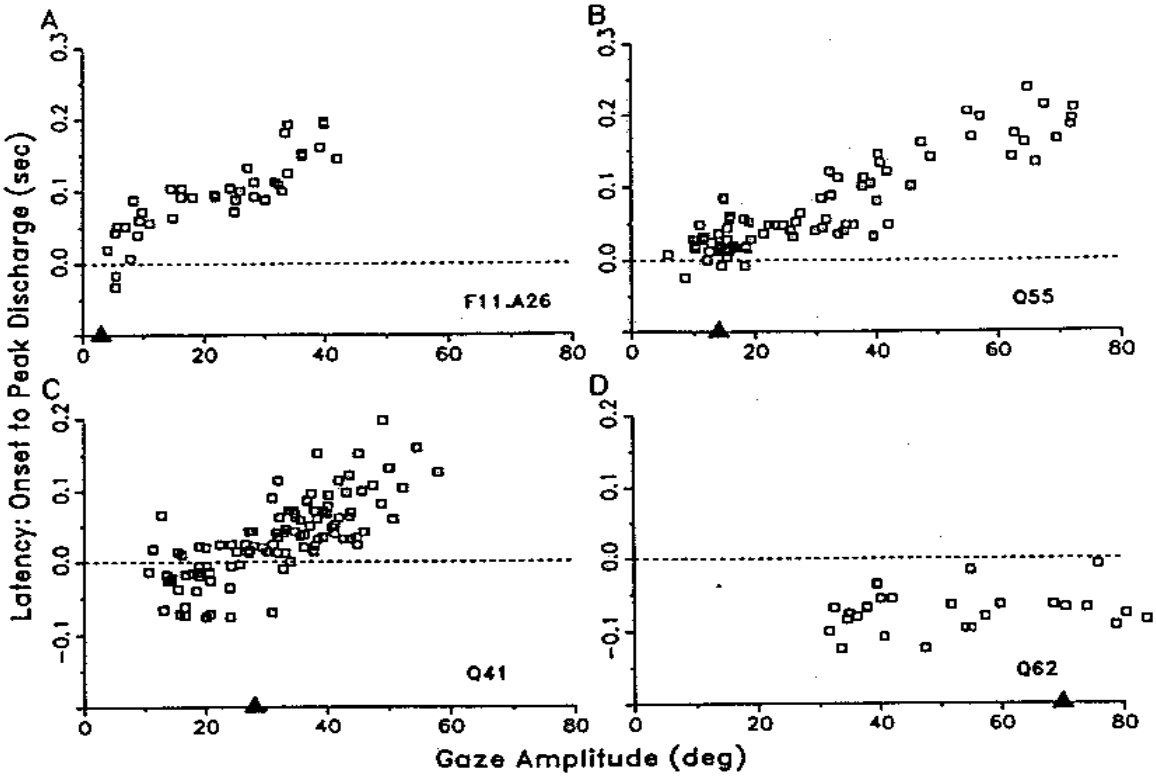

FIG. 11. Plots of latency from movement onset to peak discharge vs. overall gaze amplitude for 4 different oTR(S)Ns. Data were obtained from gaze shifts made to the predicted target when the head was unrestrained. Magnitude of the optimal gaze position error vectors of the 4 cells, indicated by the filled triangles on the abscissas, are 3 (*A*), 14 (*B*), 28 (*C*), and 70° (*D*). See legend to Fig. 9 for additional details.

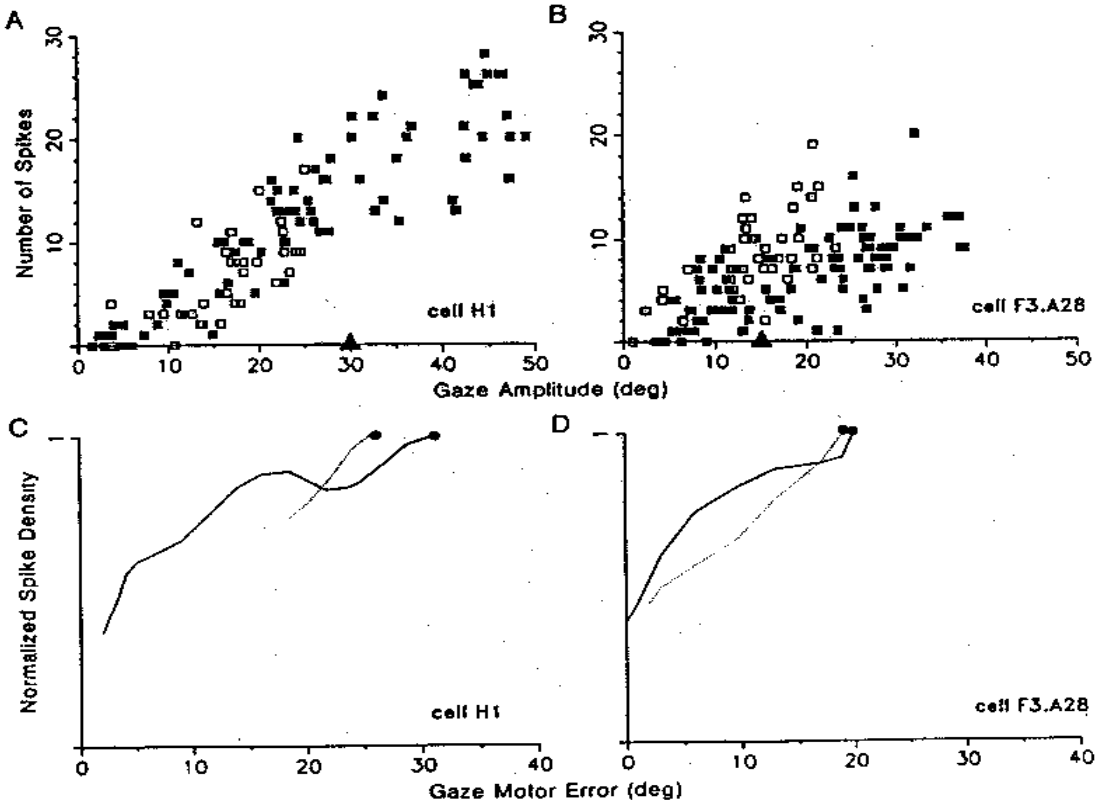

FIG. 12. Quantitative analysis of head-fixed and head-free movement fields of 2 oTR(S)Ns. *A* and *B*: plots of number of spikes (see METHODS) vs. overall gaze amplitude for head-fixed (□) and head-free (■) data. *C* and *D*: plots of normalized spike probability density function vs. instantaneous gaze motor error for the head-fixed (· · · ·) and head-free (——) conditions. See legend to Fig. 9 for additional details.

the normalized spike density functions of the two oTR(S)Ns against instantaneous gaze motor error for head-free (——) and head-fixed (· · · ·) movements. Regardless of whether the head was restrained, the neural activity recorded from these cells diminished as gaze motor error was driven toward 0°, even though, in the head-fixed condition, head motor error remained constant before, during, and after the movement. We conclude from the data presented in Figs. 7–12 that oTR(S)N activity was best correlated to instantaneous gaze motor error.

Movement-related discharges of fTR(S)Ns

We were able to study the movement-related discharge patterns of 10 fTR(S)Ns. These cells were maximally active when cats attentively fixated a food target and almost silent when the visual axis was directed away from the food (Munoz and Guitton 1991). fTR(S)Ns were only sporadically active when no food was present and the animals fixated on a blank screen. In this latter behavioral condition, there was no consistent relationship between the pattern of fTR(S)N discharge and the occurrence of spontaneous gaze shifts. However, when cats oriented using the visible food target as a cue, we did recognize a consistent pattern of fTR(S)N activity. Most notably, there was a decrease or pause in discharge associated with visually triggered movements.

Figure 13 illustrates the movement-related discharges recorded from an fTR(S)N when a head-free cat generated several rightward (Fig. 13, *A–C*) and leftward (Fig. 13, *D–F*) gaze shifts to the visible target. This neuron was located in the rostral left SC. The behavioral conditions used to obtain the data in Fig. 13 were identical to those described in relation to Fig. 4. The traces are aligned (vertical dashed line) on target disappearance (Fig. 13, *A* and *D*), onset of the gaze shift (Fig. 13, *B* and *E*), and termination of the gaze shift (Fig. 13, *C* and *F*). The histograms summarizing cell discharge show that this fTR(S)N was maximally active when the cat was attentively fixating the food target. Cell discharge frequency declined soon after target disappearance. For leftward movements in particular, the neuron was silent shortly before and during the gaze shifts. The cell's high-frequency discharge rate resumed only near the termination of the gaze shift. This resumption of fixation-related activity began just before gaze was stabilized on the target, that is, when gaze motor error was near zero.

SC uses a spatial code for instantaneous gaze motor error

The observations presented in the preceding sections suggest that during a gaze shift the peak of neural activity moved across the TR(S)N layer of the SC motor map from the initially active caudal site—specifying the amplitude and direction of the desired movement—to the rostral fixa-

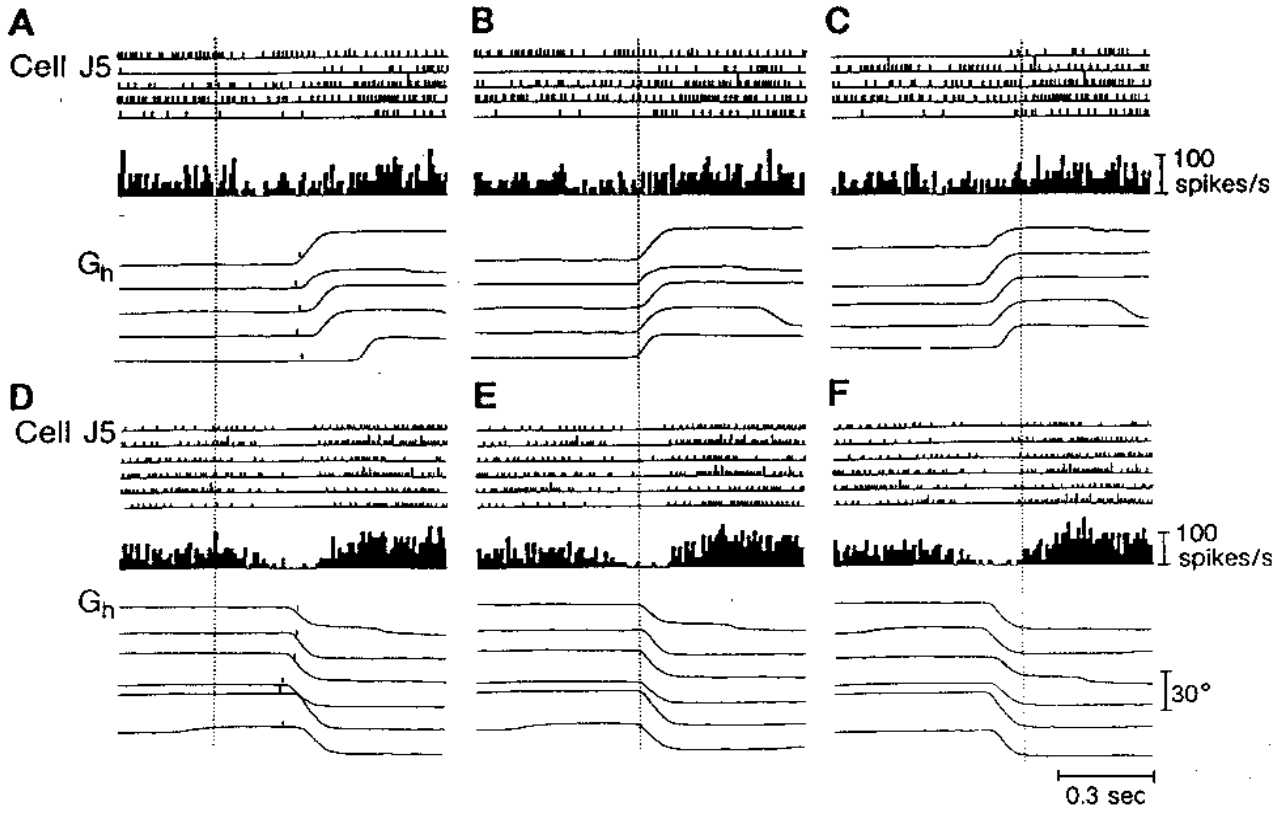

FIG. 13. Comparison of fTR(S)N discharge patterns recorded during rightward (*A–C*) and leftward (*D–F*) movements to a visible target when the head was unrestrained. Target, being fixated on one side of the barrier, disappears behind and reappears on the other side as shown in Fig. 4. Cell was located in the rostral left SC. Shown in each section are several rasters of cell discharge, a summary histogram, and the corresponding gaze position traces. Traces are aligned on target disappearance (*A* and *D*), onset of gaze shifts (*B* and *E*), and termination of gaze shifts (*C* and *F*). Tick marks *beneath* each trace in *A* and *D* indicate when target reappears from behind the barrier.

tion zone. Thus the instantaneous location of this neural activity reflected a spatial representation of instantaneous gaze motor error. At the end of the gaze shift, fTR(S)Ns, located in the rostral SC, were activated, signaling 0° gaze motor error.

To illustrate more completely this dynamic process, we present in Fig. 14 the spike density versus gaze motor error plots for several TR(S)Ns that responded optimally to various gaze position errors. The curves are plotted on retinotopic coordinates in Fig. 14*A*. The filled triangles on the abscissas in Fig. 14*A* correspond to the magnitude of each cell's optimal gaze position error vector. The cell at the top preferred the greatest amount of error, whereas the two cells located at the bottom are fTR(S)Ns. We have included responses to both ipsiversive and contraversive movements for the fixation cells. For all other cells, only contraversive movements are shown. All the data plotted in Fig. 14 were obtained from head-free recordings, except that of fTR(S)N, *cell F3.A30*, in which only head-fixed data were available. The peak of the spike density function for all cells occurred at a value of instantaneous gaze motor error that was very close to each cell's optimal gaze position error vector. This can be seen more clearly in Fig. 15, where, for 12 TR(S)Ns, we plot the magnitude of each cell's optimal gaze position error vector (derived from periods when the visual axis was stationary; see Munoz and Guitton 1991) against the magnitude of each cell's optimal instantaneous gaze motor error (derived from the spike density vs. gaze motor error plots; e.g., Fig. 14*A*). The solid line was generated from a regression analysis of the data (slope = 0.87; r = 0.99). Thus each TR(S)N was maximally active when the instantaneous position of the visual axis was directed at some vector quantity away from a target of interest, regardless of whether the gaze axis was stationary or moving toward the target.

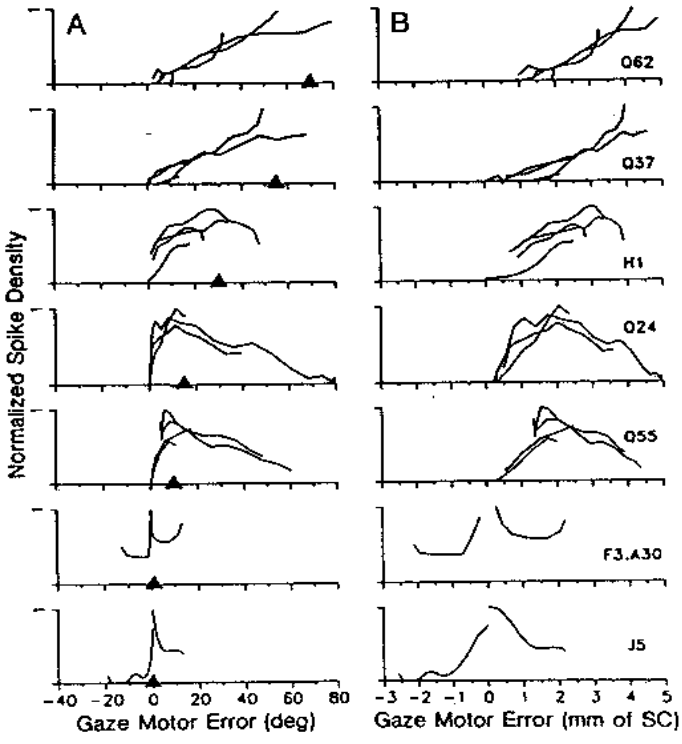

FIG. 14. Plots of spike probability density function vs. instantaneous gaze motor error for 7 TR(S)Ns. Cells are arranged, from *top* to *bottom*, on the basis of decreasing magnitude of their optimal gaze motor error. The *2 bottom cells* were classified as fTR(S)Ns. *A*: gaze motor error expressed in degrees. *B*: gaze motor error expressed as distance on collicular map.

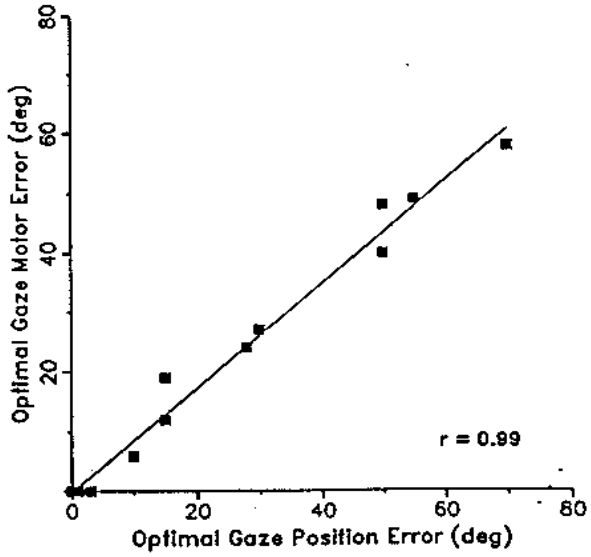

FIG. 15. Plot of optimal gaze position error (derived from periods when the visual axis was stationary; Munoz and Guitton 1991) vs. optimal gaze motor error (derived from spike density vs. gaze motor error plots; e.g., see Fig. 14*A*) for 12 TR(S)Ns.

Figure 14*A* shows that some cells (*top panels*) were active across a very wide range of gaze motor errors, whereas other cells (*bottom panels*) were active for a more restricted range of gaze motor errors. This variability in the range of gaze motor errors for which a cell is active may be due, in large part, to the nonhomogeneous mapping across the SC in which the zone devoted to the mapping of large gaze shifts is very compressed. To investigate the effect of nonlinear mapping, we plotted the spike density vs. gaze motor error curves onto the coordinate system of the cat SC (Fig. 14*B*) that we derived in the preceding paper (see Fig. 11 and *Eq. 1* of Munoz and Guitton 1991). To convert the data from retinal coordinates to collicular coordinates, we used

$$r = 0.66\theta^{0.46} \qquad (1)$$

where θ represents the value of gaze motor error in degrees and r represents the distance, in millimeters, between that value and the representation of 0° gaze motor error on the SC motor map. Note that when the spike density versus gaze motor error plots are recast onto the collicular coordinate system, the curves assume more symmetric bell-shaped trajectories. Furthermore, when we compare the different panels in Fig. 14*B*, we see that the shapes of the curves are also more similar than those in Fig. 14*A*.

Extending the arguments of McIlwain (1975, 1986), the boundary of a cell's motor field, as drawn on the coordinate system of the SC, defines the locus of all cells in that layer activated by that value of gaze motor error. The bell-shaped curves in Fig. 14*B* span some 6 mm of gaze motor error. It follows that, at any time during an orienting gaze shift, a zone of activity ~3 mm in diameter is moving across the

TR(S)N layer; its instantaneous location on the map depends on the remaining gaze motor error. Therefore the population of TR(S)Ns phasically active at any one time is very large indeed, because the cat's SC only extends up to 6 mm in the rostrocaudal dimension.

DISCUSSION

This paper presents the first comprehensive study of movement-related discharges of identified collicular output neurons in an alert animal with its head unrestrained and further implicates the cat's tectoreticulospinal pathway in the control of gaze. In the previous paper (Munoz and Guitton 1991) we identified two collicular zones with TR(S)Ns that behave in opposing fashion: the control of fixation versus that of preparing an orientating gaze shift. During the period preceding a gaze shift, when the visual axis was immobile, the vector between current and desired gaze positions (gaze position error) was represented by the spatial distribution of low-level TR(S)N sustained activity on the SC motor map. In this paper we presented two key observations critical to the understanding of how this spatially coded information is transformed into a motor command. *1*) The intensity of oTR(S)N burst discharges influenced the speed of a gaze trajectory: a sudden increase in the firing frequency of oTR(S)Ns led to the short-latency acceleration of eye and head motion. *2*) During the course of an orienting gaze shift, the zone of TR(S)N phasic activity migrated through the TR(S)N layer of the SC motor map toward the rostral fixation zone. Its instantaneous location on the map was correlated to instantaneous gaze motor error.

To discuss this material, we first consider the movement-related discharges of oTR(S)Ns and fTR(S)Ns in the context of other studies describing collicular movement-related activity. Then we discuss the role of the tectoreticulospinal pathway in providing the brain stem premotor circuitry with signals necessary for the control of both eye and head orienting movements. Finally, we present a novel scheme showing how TR(S)Ns, lying within a gaze feedback loop, may exert control over the eye and head motor systems.

oTR(S)Ns

RELATIONSHIP TO OTHER CAT STUDIES. The observations we present here are compatible with other descriptions of oTR(S)N movement-related activity recorded in alert cats (Berthoz et al. 1986; Grantyn and Berthoz 1985). These authors reported that TRSNs recorded in the head-fixed cat discharged high-frequency bursts of action potentials before visually triggered saccades and accompanying bursts in the dorsal neck muscle EMG. This activity was absent for spontaneously generated saccades. We found that some TR(S)Ns occasionally discharged a few action potentials before spontaneous movements. These discharges were much weaker than those associated with visually triggered gaze shifts. Furthermore, the peak gaze velocity was usually much lower for spontaneous than for visually triggered movements.

Other studies describing the discharges of randomly sampled, unidentified neurons recorded from the deeper collicular laminae of alert cats have reported that only a small percentage had any pre- or per-movement activity (Harris 1980; Peck 1987, 1990; Peck et al. 1980; Straschill and Schick 1977). The description of these unidentified movement-related neurons is consistent with some of the characteristics of oTR(S)N movement-related discharge. Specifically, these authors described neuronal discharges related to the initiation of eye and/or head movements. These discharge patterns typically consisted of increased activity for movements of a specific amplitude and direction that defined a movement field. None of these studies, however, reported cells with exclusively open-ended movement fields or correlations to instantaneous gaze motor error.

RELATIONSHIP TO MONKEY STUDIES. Several different saccade-related activity patterns have been described for unidentified neurons encountered in the deeper collicular laminae of the alert, head-fixed monkey (Mays and Sparks 1980; Mohler and Wurtz 1976; Schiller and Koerner 1971; Schiller and Stryker 1972; Sparks 1975, 1978; Sparks et al. 1976; Sparks and Mays 1980; Wurtz and Goldberg 1971, 1972a). One class of neuron, the SRBN, discharges a high-frequency burst of action potentials immediately before saccades made in either the light or dark (Schiller and Koerner 1971; Sparks et al. 1976; Wurtz and Goldberg 1971, 1972a). This burst precedes saccades of a specific amplitude and direction by ~20 ms, and its occurrence is almost perfectly correlated to the occurrence of the saccade (Sparks 1978). Because at least some of these neurons have been antidromically activated from the paramedian pontine reticular formation (Keller 1979), it has been suggested (Sparks and Mays 1981) that they serve as a trigger input to the pontine premotor circuitry that must generate the saccadic burst signal. Another class of movement-related neuron found in the primate SC is the visually triggered movement cell (VTMC), which increases its discharge rate before visually triggered, but not spontaneous, saccades (Mohler and Wurtz 1976). A third class of movement-related neuron found in the primate SC is the quasivisual (QV) cell, which presents a sustained discharge for a given eye position error (Mays and Sparks 1980).

Although there are some major differences (discussed below) between cat oTR(S)Ns and saccade-related cells recorded in the head-fixed monkey, the discharge pattern of the typical cat oTR(S)N combines some of the attributes of monkey SRBNs, QV cells, and VTMCs. Like QV cells, TR(S)Ns had sustained preamble discharges that signaled the presence of a gaze position error. Almost all TR(S)Ns were maximally active before visually triggered movements, which is characteristic of monkey VTMCs. However, some TR(S)Ns also increased their rate of discharge for predictive and spontaneous movements, an attribute of the SRBN. Our results suggest that it is artificial to group TR(S)Ns into different response categories. Rather, this collicular efferent neuron can be considered to carry all of the above signals, but with different gains, such that for any given cell one or more of the movement-related discharge patterns becomes dominant.

MOVEMENT FIELDS. It has been reported that a given SRBN, recorded in the head-fixed monkey, discharges with a vigorous burst before saccades of a specific direction and amplitude that define a movement field (Mohler and Wurtz 1976; Schiller and Koerner 1971; Sparks et al. 1976; Wurtz and Goldberg 1971, 1972a). The intensity of this response diminishes when the saccade trajectory deviates

from the cell's optimal vector. The movement-related burst of an oTR(S)N, like that of an SRBN, was weaker when a saccade's direction deviated from the optimal. However, the relationship between cat oTR(S)N discharge and movement amplitude for movements along the optimal direction differed dramatically from monkey SRBNs. The temporal pattern of the oTR(S)N movement-related response varied systematically with gaze amplitude. For amplitudes much less than the optimal gaze position error vector, TR(S)Ns, like SRBNs, were silent. However, when movement amplitude was much greater than the optimal gaze position error vector, oTR(S)N activity, unlike that of SRBNs, did not diminish. Rather, as overall gaze amplitude increased, peak discharge was delayed relative to movement onset and occurred at the time during the movement when instantaneous gaze motor error achieved a specific value (see Figs. 7–10).

SC AND MOVEMENT VELOCITY. Our data suggest a causal link between the intensity of oTR(S)N discharge and movement velocity. *1*) The intensity of the movement-related burst of some cells covaried with movement velocity (Figs. 1–3). *2*) The velocity of eye and head movements generated by collicular microstimulation was influenced by the frequency of pulses in the train (Fig. 5). *3*) A visually or electrically evoked burst of oTR(S)N discharge led to a reacceleration in the gaze trajectory after a latency of only 10 ms (see Figs. 4 and 6 and Table 1).

Other experimental findings support the notion of collicular involvement in determining the velocity of saccadic eye movements. After total SC ablation in the monkey, saccadic eye velocity was reduced (Schiller et al. 1980; Wurtz and Goldberg 1972b). Pharmacologically induced activation or deactivation of small regions of the monkey SC also affect saccade velocity (Hikosaka and Wurtz 1985, 1986; Lee et al. 1988). Berthoz and co-workers (1986), experimenting in the head-fixed cat, first reported that the shape of TRSN burst profiles closely matched saccadic eye velocity profiles. These authors reported latencies of 50 ms between burst and saccade onsets when the cat oriented toward a moving visual stimulus. Recent single-unit recordings from SRBNs in the monkey have also yielded discharges with intensities that are related to the velocity of saccades (Rohrer et al. 1987).

RELATIONSHIP TO ANATOMY. On the basis of morphological criteria, two major classes of collicular efferent neurons projecting an axon into the predorsal bundle have been described (for review see Guitton 1991) in both the cat (Moschovakis and Karabelas 1985) and monkey (Moschovakis et al. 1988a). "X" cells have large somas that give rise to a single, thick axon that projects into the contralateral predorsal bundle. Some ipsilateral collaterals are also distributed to mesencephalic regions implicated in eye-movement control. "T" cells, on the other hand, are considerably smaller in size and give rise to thin axons. Their axonal projections include recurrent collaterals that terminate near the parent soma; a tectal commissural fiber; and, in some cells, a projection into a tectal efferent bundle (e.g., the predorsal bundle). Combined morphological and physiological studies of SRBNs in the alert, untrained squirrel monkey have revealed that they do indeed project an axon into the predorsal bundle (Moschovakis et al. 1988b). On the basis of soma and axon size and their pattern of axonal arborization, these authors concluded that monkey SRBNs are a subset of T neurons. The discharge characteristics of monkey X cells remains obscure.

All of the TR(S)N response types illustrated in this series of papers were recorded from fast conducting neurons. On the basis of estimates of conduction velocity (Guitton and Munoz 1991), these fit the category of X cells described by Moschovakis and Karabelas (1985). These authors also reported that, in the cat, very few T cells projected into the contralateral predorsal bundle. Therefore, in the cat, collicular information related to the execution of movement must presumably be carried by X cells to the brain stem premotor circuitry.

fTR(S)Ns

This study is the first to demonstrate that signals related to the maintenance of visual fixation are relayed through the SC to the brain stem premotor circuitry via fTR(S)Ns. Fixation TR(S)Ns were tonically active when a cat attentively fixated a target of interest and reduced their rate of discharge before and during orienting gaze shifts. These discharge characteristics are similar to those described for unidentified collicular neurons recorded in alert, head-fixed cats (Peck 1989) and monkeys (Goldberg and Wurtz 1971; Munoz et al. 1990; Sparks and Mays 1980). These unidentified fixation-related cells also discharged tonically when the visual axis was aligned with a target of interest and paused for saccadic eye movements.

It has recently been demonstrated that an intact SC is essential for the generation of express saccades (Schiller et al. 1987). The occurrence of these reflexlike, short-latency eye movements has been linked to the interruption of active, or attentive, fixation before target appearance (Boch and Fischer 1986; Fischer and Boch 1983; Fischer and Rampsberger 1984; Munoz 1988). We propose that silencing of fTR(S)Ns is a prerequisite for the generation of express saccades and that classic visually triggered movements have longer latencies largely because of the time it takes to silence fixation activity in the SC and possibly elsewhere, such as in the frontal (Bruce and Goldberg 1985; Segraves and Goldberg 1987) and parietal (Lynch et al. 1977; Sakata et al. 1980) lobes.

TR(S)Ns provide a common drive to the eye and head

Before the initiation of this study, evidence had accumulated suggesting that the cat SC may be involved in coordinating eye-head orienting behavior. Stimulation of the SC in anesthetized cats produced disynaptic excitatory postsynaptic potentials in contralateral abducens (Grantyn and Grantyn 1976) and dorsal neck (Anderson et al. 1971) motoneurons. Stimulation of the SC in alert cats triggered coordinated eye-head orienting movements (Roucoux et al. 1980) that were very similar to naturally occurring eye-head orienting movements. Intra-axonal injection of horseradish peroxidase into TRSNs revealed their extensive pattern of collateralization (Grantyn and Grantyn 1982) to many brain stem regions implicated in the control of eye and head movement.

We have proposed that the eye and head premotor circuitry are driven by a common signal because of the high degree of covariability in the eye and head components of

natural gaze shifts made by cats (Guitton et al. 1990). TR(S)Ns appear to provide at least part of the common drive to the eye and head premotor circuitry. *1*) TR(S)Ns had similar movement-related discharge patterns in both head-fixed and head-free conditions (Figs. 9–12 and 14), provided the target was within the animal's oculomotor range. *2*) The intensity of some oTR(S)N movement-related discharges (Fig. 3) and the frequency of collicular stimulation (Fig. 5 and Table 2) were correlated to the velocity of both eye and head components of gaze shifts. *3*) Burst discharges of oTR(S)Ns, or bursts of microstimulation imposed in the middle of gaze shifts, led to short-latency reacceleration of both the eyes and head at minimal latencies (Figs. 4 and 6 and Table 1). *4*) TR(S)N spike density functions were best correlated to instantaneous gaze motor error (Figs. 9, 10, and 12).

Previous single-unit recording studies describing neural discharges in the SC of alert, head-free animals have failed to reveal a role for the SC in gaze control. Straschill and Schick (1977) and Harris (1980), recording in the head-free cat SC, found some cells that discharged before eye movements and others that fired before head movement. More recently, Peck (1990) reported that cells discharging before head movements also discharged before eye movements. None of these studies, however, found cells for which discharge was tightly correlated to gaze. Robinson and Jarvis (1974), recording in the SC of head-free monkeys, found no neurons in the intermediate layers that discharged in relation to head movements. They found that neuronal activity had a better temporal relation to saccadic eye movements. However, in their experimental paradigm, most of the gaze shifts had amplitudes well within the monkey's oculomotor range, which required little or no head movement (Tomlinson and Bahra 1986). In this context, it would be of considerable interest to explore the more posterior aspects of the monkey SC, where larger gaze shifts are represented.

Spatial representation of instantaneous gaze motor error

The direction and amplitude of a saccade are thought to be represented by the spatial distribution of activity on the SC motor map (Lee et al. 1988; McIlwain 1982; Sparks et al. 1976; van Gisbergen et al. 1987; van Opstal and van Gisbergen 1990). It is currently believed that each collicular output neuron specifies a vector, the amplitude and direction of which are determined by the cell's location on the motor map. The brain stem premotor circuitry generates a movement of the appropriate amplitude and direction by calculating, from all the activity on the SC motor map, the weighted vector average. The deviation in saccade trajectory that follows inactivation of small regions of the SC can be accounted for by the absence of certain vector contributions from the weighted vector average (Lee et al. 1988).

The data presented here suggest that the cat SC maintains a spatial representation of gaze motor error not only before movement onset but also during the execution of the gaze shift. The following points support this conclusion. *1*) All oTR(S)Ns that we studied were active for movements in the optimal direction when the magnitudes of the movements were equal to or greater than the cell's optimal gaze position error vector (Figs. 7–12). That is, these cells had open-ended movement fields. *2*) The timing of a cell's discharge relative to the onset and termination of the movement was dependent on the overall magnitude of the gaze displacement. *3*) Each oTR(S)N achieved peak discharge for a specific value of gaze motor error, regardless of overall movement amplitude (Figs. 9–12, and 14). *4*) For movements generated with the head unrestrained, plots of spike density versus instantaneous eye motor error revealed weaker overlaps than plots of spike density versus instantaneous gaze motor error (Figs. 9, *J–L* and 10, *J–L*). *5*) Similar plots of spike density versus instantaneous gaze motor error were obtained in the head-fixed and head-free conditions (Fig. 12), thereby eliminating the possibility that instantaneous head motion was being controlled. We conclude that instantaneous gaze motor error is topographically represented by TR(S)Ns.

An alternative interpretation to the data is that a circular wave of activity propagates in a radial direction from an origin at the initial site of activation. Our data are not compatible with this mechanism. There was a lack of burst activity in TR(S)Ns located caudal to the initially active zone. For example, cell Q37 did not burst (Fig. 8*A*) after the start of 10–15° gaze shifts that began at the site of cell Q24 (Fig. 7, *A* and *B*).

Although our data constitute the first compelling evidence for displacement of neuronal activity on the SC motor map during a gaze shift, this idea is not new. A network to do this was first formally presented by Pitts and McCullough (1947). Other models of visuooculomotor transformation, based on the principle that activity is displaced on a motor map, have been proposed (Droulez and Berthoz 1988, 1991; Eckmiller 1988; Lefevre and Galiana 1990; and Tweed and Vilis 1985).

Conceptual scheme to describe TR(S)N control of orienting behavior

In this final section we integrate the findings presented in this and the accompanying papers (Guitton and Munoz 1991; Munoz and Guitton 1991) into a conceptual framework that describes the role of TR(S)Ns in the control of orienting behavior in the cat. In Fig. 16*A* we present a schema that incorporates TR(S)Ns into a gaze feedback loop that drives the oculomotor and head motor systems.

RELATIONS WITH PREMOTOR CIRCUITRY. Regarding the genesis of horizontal eye movements, several different types of neurons in the paramedian pontine reticular formation have been implicated in controlling oculomotor behavior in both the cat and monkey (for review see Fuchs et al. 1985; Keller 1979; Robinson 1975; Scudder 1988). Excitatory burst neurons (EBNs) discharge high-frequency bursts of action potentials immediately before saccadic eye movements. EBNs project monosynaptically onto extraocular muscle motoneurons, providing an important signal required to drive the saccade (Strassman et al. 1986). During intersaccade intervals, EBNs are inhibited by tonically active omnipause neurons (OPNs), which, in turn, pause immediately before a saccade, thereby disinhibiting the EBNs (Curthoys et al. 1984). Another premotor neuron implicated in saccade initiation is the long-lead burst neuron (LLBN), the burst activity of which, before a saccade, pre-

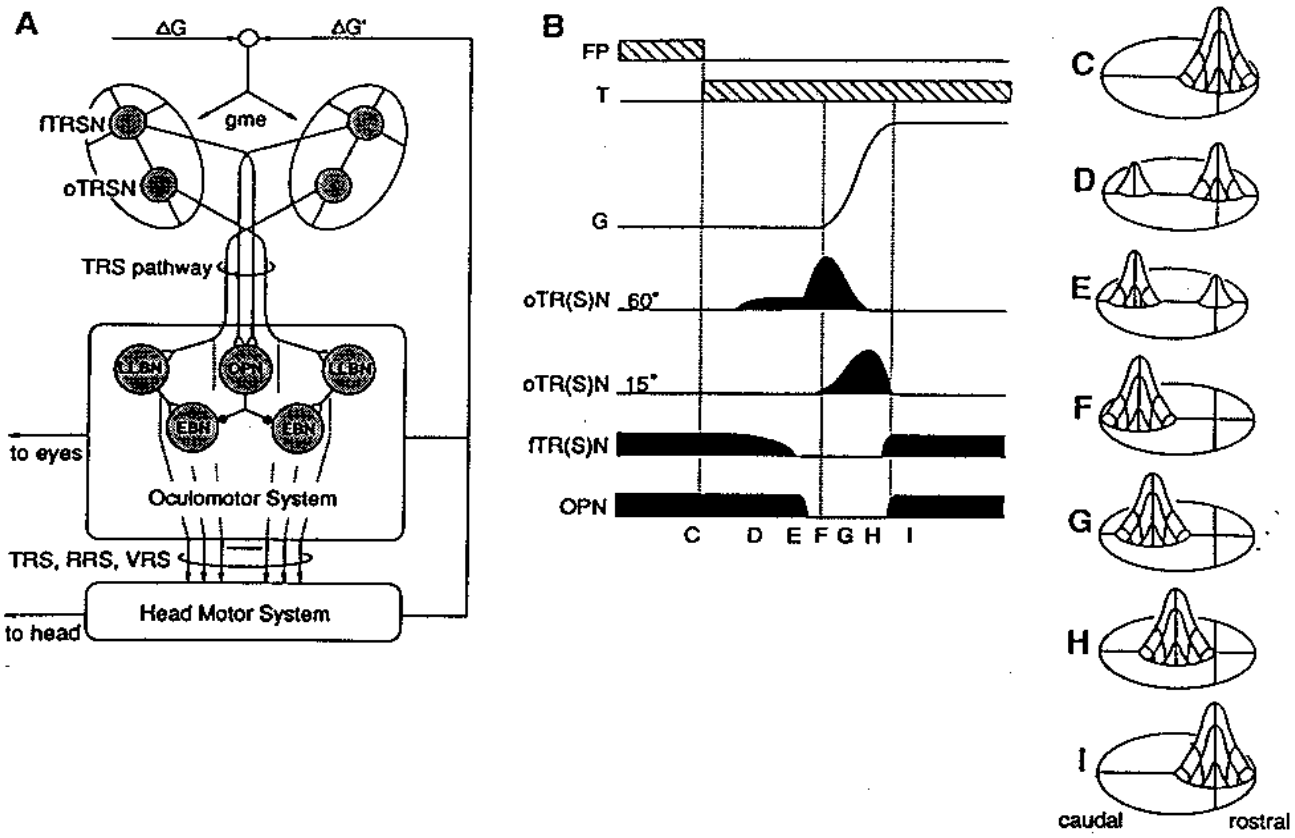

FIG. 16. *A*: proposed links between SC and brain stem oculomotor circuitry. Schematized dorsal view of the left and right SC is shown at *top*. Two axons leave each colliculus. Cell body of one, a fTR(S)N, is situated in the area centralis representation (where the 2 solid axes intersect) and projects to omnipause neurons (OPNs). The other, an oTR(S)N, originates from a more caudal site and projects to long-lead burst neurons (LLBNs). LLBNs and OPNs then terminate monosynaptically onto excitatory burst neurons (EBNs). Excitatory connections are drawn as open triangles, whereas inhibitory connections are denoted by filled circles. Tectoreticulospinal (TRS) system, in conjunction with reticuloreticulospinal (RRS) and vestibuloreticulospinal (VRS) networks, also projects to the head motor system, the contents of which are left blank. Outputs of the eye and head motor systems sum to yield an internal representation of change in gaze position (ΔG'). This signal is subtracted from desired change in gaze position (ΔG) to yield instantaneous gaze motor error (gme), which is topographically represented on the SC motor map. *B*: schematized discharge patterns of various neurons in the illustrated circuit when a cat, with its gaze (G) first directed toward a fixation point (FP), orients to a target (T) 60° in the periphery. Dashed line on *left* indicates offset of FP and onset of T. *Middle* and *right* dashed lines indicate the start and end of gaze shift. Shown are the discharge patterns of an oTR(S)N for which the optimal gaze motor error is 60° in amplitude, an oTR(S)N for which the optimal gaze motor error is 15° in amplitude, an fTR(S)N, and an OPN. Letters *under* the OPN trace correspond to times when the spatial distribution of TR(S)N activity matches that illustrated in *C–I*. *C–I*: proposed activity patterns in the TR(S)N layer of the SC when the cat fixates a target of interest (*C–E*) and then orients to a new target of interest (*F–I*). Neural activity (firing frequency) is represented schematically as a hill protruding out of the motor map. Zero position on the map is at the intersection of the horizontal and vertical meridians in the rostral pole.

cedes that of the EBN (Curthoys et al. 1981; Keller 1974; Luschei and Fuchs 1972).

In both cat (Grantyn et al. 1988) and monkey (Raybourn and Keller 1977), LLBNs receive a powerful, monosynaptic excitatory input from the SC. The LLBN discharge pattern preceding a saccadic eye movement is similar to that of oTR(S)Ns. LLBNs discharge a low-frequency prelude, the onset latency of which relative to the saccade is extremely variable. We postulate that the discharges of oTR(S)Ns directly activate LLBNs, which, in turn, attempt to drive the EBNs. However, only when there is a cessation in OPN discharge can the EBN be activated.

fTR(S)Ns located in the rostral SC are active during attentive fixation, a behavioral condition in which orientation is suppressed. What is the brain stem destination of this fixation-related signal? Raybourn and Keller (1977) found that, in the alert monkey, OPNs were monosynaptically activated by electrically stimulating the SC. This was also reported for OPNs recorded in the anesthetized cat (King et al. 1980). Several discharge properties of cat OPNs are similar to fTR(S)Ns. Both cell types pause for orienting gaze shifts; however, OPNs pause for movements of all amplitudes and directions (Evinger et al. 1982; Paré and Guitton 1990), whereas the pause of fTR(S)Ns is sometimes incomplete (see Figs. 13 and 14). Evinger and co-workers (1982) reported that OPNs, like fTR(S)Ns, respond to visual, auditory, and somatosensory stimuli; their visual receptive fields are large and always contain a representation of the area centralis. Furthermore, the tonic rate of discharge of both fTR(S)Ns (Munoz and Guitton 1991) and OPNs decreases when the cat is in the dark, not performing visuomotor tasks. We propose that fTR(S)Ns activate

OPNs and/or analogous premotor elements that are involved in suppressing movement. Sparks and Mays (1983) and Peck (1989) have also proposed that collicular fixation neurons project onto OPNs.

In the schema presented in Fig. 16*A*, TR(S)Ns in both the rostral and caudal SC are shown to project on the oculomotor and head motor systems via the tectoreticulospinal pathway. We have incorporated the connections of fTR(S)Ns onto OPNs and oTR(S)Ns onto LLBNs. These projections need not be exclusive; that is, both fixation and orientation TR(S)Ns may project onto both OPNs and LLBNs, with the efficacy of these connections varying reciprocally in the rostrocaudal direction.

Very little is known about the premotor circuitry that controls rapid orientation of the head. We have proposed elsewhere that the head motor system is driven by both gaze motor error and the extraocular motoneuronal signal (Guitton et al. 1990). These inputs into the head motor system are shown, in Fig. 16*A*, to be carried by *1*) TR(S)Ns; *2*) LLBNs that receive monosynaptic collicular inputs and project to both the brain stem reticular formation and spinal cord (Grantyn et al. 1988; Peterson 1977; Scudder et al. 1989); and *3*) burst-tonic cells in the vestibular nuclei and adjacent reticular formation that carry extraocular motoneuron signals and that also project to the brain stem reticular formation and spinal cord (Grantyn and Berthoz 1987; Grantyn et al. 1987, 1988; McCrea et al. 1987; Peterson 1977). These pathways have been labeled tectoreticulospinal (TRS), reticuloreticulospinal (RRS), and vestibuloreticulospinal (VRS) in Fig. 16*A*.

ROLE OF THE SC IN THE FEEDBACK CONTROL OF GAZE SHIFTS. Many models of the SC–brain stem burst generator system have been proposed. These models can be grouped into two classes (reviewed by Guitton 1991): *1*) those in which the SC signal functions open loop and specifies only the initial vector of motor error (e.g., see Scudder 1988; Tweed and Vilis 1990) and *2*) those in which the SC lies within a feedback loop and specifies the instantaneous motor error vector (e.g., see Keller 1981; Waitzman et al. 1988). Our data support the second category.

Keller (1981) first proposed that the SC is within the feedback loop controlling saccades. He utilized elements of the Robinson (1975) "local feedback" model, incorporating them within the SC and brain stem circuitry. Thus the locus of activity within the SC, specifying motor error, was the result of eye position and target position signals feeding back on the SC. Motor error, the collicular output, was passed to the burst generator. This view is in contradiction to a recent model by Scudder (1988) in which the colliculus acts open loop and provides the burst generator with an initial command specifying the size and direction of the appropriate saccade.

Waitzman and co-workers (1988) recently demonstrated that the discharge of SRBNs, located in the monkey SC, decreased during head-fixed saccades, in proportion to instantaneous eye motor error. They concluded that these cells are within the feedback loop that control saccades. Feedback, in their model, flattens a "hill" of neural activity that remains stationary on the motor map.

Many studies have proposed that, during the execution of coordinated eye-head orienting movements, gaze accuracy is achieved by means of a gaze feedback loop (reviewed and modeled in Guitton et al. 1990). The present findings suggest that the topographically coded signal of instantaneous gaze motor error in the TR(S)N layer of the SC may constitute part of this gaze feedback loop. In the schema presented in Fig. 16*A*, a signal related to the change in gaze position ($\Delta G'$) is returned to the SC. This signal could be derived from a resettable integrator that would integrate the gaze velocity command (Jurgens et al. 1981). Alternatively, eye and head velocity commands could be independently integrated and combined to produce the $\Delta G'$ signal. Regardless of its genesis, the $\Delta G'$ signal is subtracted from the original retinal error signal specifying desired change in gaze position (ΔG) to yield instantaneous gaze motor error (gme), which is sent by the tectoreticulospinal pathway to the eye and head premotor circuitry.

The feedback hypothesis illustrated in Fig. 16*A* is supported by observations that the intensity of oTR(S)N bursts influences gaze velocity and that sudden increases in the discharge frequency of oTR(S)N phasic bursts speed up gaze shifts without affecting their accuracy. These findings are difficult to reconcile with current models that place the SC upstream of the local feedback loop. If, however, the SC were inside the feedback loop and provided the error signal, then higher velocity movements would eliminate gaze error more quickly such that movement duration would be shorter and accuracy would be maintained.

PROPOSED SPATIOTEMPORAL TRANSFORMATION. The schema presented in Fig. 16*A* illustrates one way in which a topographically represented motor command can be transformed into the temporal firing pattern that motoneurons send to muscles (the so-called spatiotemporal transformation) by driving gaze throughout the spatial trajectory of neural activity on the SC motor map. This is schematically shown in Fig. 16, *B–I*, where we illustrate the sequence of events in the SC when a cat generates a 60° gaze shift to a target that unexpectedly appears in the periphery. The four neurons for which discharges are schematized in Fig. 16*B* are, from *top* to *bottom*, an oTR(S)N located at the 60° representation, an oTR(S)N located at the 15° representation, a fTR(S)N located in the rostral SC, and an OPN. Figure 16, *C–I*, shows the spatial distribution of activity in the TR(S)N layer of the SC related to the preparation and execution of the hypothesized movement. Neural activity is represented as a hill protruding from the surface of the motor map. The height of the hill corresponds to the intensity of that activation.

First, while the cat attends to a fixation point, fTR(S)Ns in both rostral poles are active and TR(S)Ns located elsewhere on the map are silent. Accordingly, we have centered TR(S)N activity on the zero error representation of the SC motor map (Fig. 16*C*). We proposed that activity at zero inhibits the rest of the SC. This mechanism would make it harder for any sensory input to activate oTR(S)Ns in the more caudal colliculus. Furthermore, as proposed above, the discharge of the OPNs would be higher during attentive fixation. This combination of increased OPN activity and decreased excitability of oTR(S)Ns in the caudal SC would reduce the probability of triggering an orienting movement.

After appearance of the target, an ensemble of oTR(S)Ns, the average gaze position error vector of which corresponds to the vector of the gaze shift required to fixate the target, is activated with a sustained discharge. This new

active zone is generated by visual inputs to the SC. If the target is located 60° to the right of the point of fixation, the new active zone would appear in the caudal left SC (Fig. 16*D*). The level of activation at the caudal locus depends on several factors, such as diligence of fixation (i.e., level of activity within the rostral fixation zone) and whether the target is defined by sensory (i.e., visual) and/or anticipatory cues. If either or both of the sensory and anticipatory drives are strong, then neural activity in this caudal zone of the SC will increase at the expense of all others, including the activity of fTR(S)Ns through the putative inter- and/or intracollicular inhibitory networks (for review see Munoz and Guitton 1991). As fixation activity diminishes, the new zone of activity in the caudal SC grows in intensity (Fig. 16*E*). Furthermore, the appropriate brain stem premotor circuitry (i.e., LLBNs on right side) would be depolarized, thereby increasing the probability of triggering the rightward orienting gaze shift to the target.

Eventually the rostral fixation zone is silenced, and oTR(S)Ns within the active zone in the caudal left SC burst to trigger the movement (Fig. 16*F*). The OPNs are silenced and the appropriate burst neurons (LLBNs and EBNs on the right side) begin to burst to drive the movement. As the eye and head movements progress, the distance between the visual axis and the target diminishes. The feedback loop shown in Fig. 16*A* alters the spatial distribution of active output neurons and the zone of TR(S)N activity moves continuously towards the rostral pole (Fig. 16, *G* and *H*). The instantaneous location of the active zone provides an internal representation of remaining gaze motor error.

If one imagines a recording microelectrode located at the 15° amplitude site on the retinotopic map, then the recorded activity would produce data similar to that in Figs. 7 and 9 (cell Q24). By comparison, a microelectrode at the 60° amplitude site would produce data similar to that in Figs. 8 and 10 (cell Q37).

As the gaze shift terminates (i.e., gaze motor error approaches zero), the active zone invades the rostral poles, where fTR(S)Ns are located (Fig. 16*I*). If the efficacy of fTR(S)N and oTR(S)N projections onto OPNs and LLBNs are appropriately weighted, then, during the course of the movement, LLBN excitability diminishes while OPN excitability increases. As OPN tonic discharge rate is reinstated, the EBNs are silenced, and the gaze saccade is terminated. The head may still continue to move toward the target, driven by an eye position signal (Guitton et al. 1990). During this latter portion of the head movement, the eye, driven by the vestibuloocular reflex, counterrotates, and gaze remains on target.

The scheme proposed in Fig. 16 has important implications regarding the role of burst neurons and OPNs in gaze control. Because the collicular output, at least in the cat, appears to drive gaze (i.e., eye plus head), some LLBNs, EBNs, and OPNs may have their discharges correlated to gaze rather than movements of the eyes alone. Indeed, recent experimental results in the cat (Paré and Guitton 1990) have shown that OPNs pause for the duration of gaze shifts rather than for the duration of saccades.

We are grateful to Dr. R. M. Douglas (Dept. of Ophthalmology, University of British Columbia, Vancouver, Canada), who wrote the computer software and contributed extensively to the installation and development of our computing facility. The technical assistance of M. Feran, M. Mazza, and J. Roy is also acknowledged.

This work was supported by the Medical Research Council (MRC) of Canada and le Fonds de la Recherche en Santé du Québec. D. P. Munoz was supported by an MRC studentship and a Natural Sciences and Engineering Research Council fellowship. D. Pélisson was supported by an MRC fellowship.

Present addresses: D. P. Munoz, Laboratory of Sensorimotor Research, National Eye Institute, National Institutes of Health, Bldg. 10, Room 10C101, Bethesda, MD 20892; D. Pélisson, Vision et Motricite, INSERM U-94, 16 av. du Doyen Lepine, 69500 Bron, France.

Address for reprint requests: D. Guitton, Montreal Neurological Institute, 3801 University St., Montréal, Québec H3A 2B4, Canada.

Received 31 January 1989; accepted in final form 11 July 1991.

REFERENCES

ANDERSON, M. E., YOSHIDA, M., AND WILSON, V. J. Influence of superior colliculus on cat neck motoneurons. *J. Neurophysiol.* 34: 898–907, 1971.

BERTHOZ, A., GRANTYN, A., AND DROULEZ, J. Some collicular efferent neurons code saccadic eye velocity. *Neurosci. Lett.* 72: 289–294, 1986.

BOCH, R. AND FISCHER, B. Further observations on the occurrence of express-saccades in the monkey. *Exp. Brain Res.* 63: 487–494, 1986.

BRUCE, C. J. AND GOLDBERG, M. E. Primate frontal eye fields. I. Single neurons discharging before saccades. *J. Neurophysiol.* 53: 603–635, 1985.

CROMMELINCK, M., PARÉ, M., AND GUITTON, D. Gaze shifts evoked by superior colliculus stimulation in the alert cat. *Soc. Neurosci. Abstr.* 16: 1082, 1990.

CURTHOYS, I. S., MARKHAM, C. H., AND FURUYA, N. Direct projection of pause neurons to nystagmus-related excitatory burst neurons in the cat pontine reticular formation. *Exp. Neurol.* 83: 414–422, 1984.

CURTHOYS, I. S., NAKAO, S., AND MARKHAM, C. H. Cat medial pontine reticular neurons related to vestibular nystagmus: firing pattern, location and projection. *Brain Res.* 222: 75–94, 1981.

DROULEZ, J. AND BERTHOZ, A. Spatial and temporal transformations in visuo-motor coordination. In: *Neural Computers*, edited by R. Eckmiller and Ch. v. d. Malsburg. Berlin: Springer-Verlag, 1988, p. 345–357.

DROULEZ, J. AND BERTHOZ, A. A neural network model of sensoritopic maps with predictive short term memory. *Proc. Natl. Acad. Sci. USA*. In press.

ECKMILLER, R. Neural networks for motor program generation. In: *Neural Computers*, edited by R. Eckmiller and Ch. v. d. Malsburg. Berlin: Springer-Verlag, 1988, p. 359–370.

EVINGER, C., KANEKO, C. R. S., AND FUCHS, A. Activity of omnipause neurons in alert cats during saccadic eye movements and visual stimuli. *J. Neurophysiol.* 45: 827–844, 1982.

FELDON, S., FELDON, P., AND KRUGER, L. Topography of the retinal projection upon the superior colliculus of the cat. *Vision Res.* 10: 135–143, 1970.

FISCHER, B. AND BOCH, R. Saccadic eye movements after extremely short reaction times in the monkey. *Brain Res.* 260: 21–26, 1983.

FISCHER, B. AND RAMPSBERGER, E. Human express saccades: extremely short reaction times of goal directed eye movements. *Exp. Brain Res.* 57: 191–195, 1984.

FUCHS, A. F., KANEKO, C. R. S., AND SCUDDER, C. A. Brainstem control of saccadic eye movements. *Annu. Rev. Neurosci.* 8: 307–337, 1985.

GOLDBERG, M. E. AND WURTZ, R. H. Response of single cells in monkey superior colliculus during pursuit eye movements and stationary fixation (Abstract). *Neurology* 21: 435, 1971.

GRANTYN, A. AND BERTHOZ, A. Burst activity of identified tecto-reticulospinal neurons in the alert cat. *Exp. Brain Res.* 57: 417–421, 1985.

GRANTYN, A. AND BERTHOZ, A. Reticulo-spinal neurons participating in the control of synergic eye and head movements during orienting in the cat. I. Behavioral properties. *Exp. Brain Res.* 66: 339–354, 1987.

GRANTYN, A. A. AND GRANTYN, R. Synaptic actions of tectofugal pathways on abducens motoneurons in the cat. *Brain Res.* 105: 269–285, 1976.

GRANTYN, A. AND GRANTYN, R. Axonal patterns and sites of termination of cat superior colliculus neurons projecting in the tecto-bulbo-spinal tract. *Exp. Brain Res.* 46: 243–256, 1982.

GRANTYN, A., HARDY, O., AND BERTHOZ, A. Activity and ponto-bulbar

connections of reticulo-spinal neurons subserving visually triggered orienting eye and head movements. *Soc. Neurosci. Abstr.* 14: 956, 1988.

GRANTYN, A., ONG-MEANG JACQUES, V., AND BERTHOZ, A. Reticulospinal neurons participating in the control of synergic eye and head movements during orienting in the cat. II. Morphological properties as revealed by intra-axonal injections of horseradish peroxidase. *Exp. Brain Res.* 66: 355–377, 1987.

GUITTON, D. Control of saccadic eye and gaze movements by the superior colliculus and basal ganglia. In: *Vision and Visual Dysfunction. Eye Movements*, edited by R. H. S. Carpenter. London: Macmillan. In press.

GUITTON, D., DOUGLAS, R. M., AND VOLLE, M. Eye-head coordination in cats. *J. Neurophysiol.* 52: 1030–1049, 1984.

GUITTON, D. AND MUNOZ, D. P. Control of orienting gaze shifts by the tectoreticulospinal system in the head-free cat. I. Identification, localization, and effects of behavior on sensory responses. *J. Neurophysiol.* 66: 1605–1623, 1991.

GUITTON, D., MUNOZ, D. P., AND GALIANA, H. L. Gaze control in the cat: studies and modeling of the coupling between orienting eye and head movements in different behavioral tasks. *J. Neurophysiol.* 64: 509–531, 1990.

GUITTON, D. AND VOLLE, M. Gaze control in humans: eye-head coordination during orienting movements to targets within and beyond the oculomotor range. *J. Neurophysiol.* 58: 427–459, 1987.

HARRIS, L. R. The superior colliculus and movements of the head and eyes in cats. *J. Physiol. Lond.* 300: 367–391, 1980.

HESS, W. R., BURGI, J., AND BUCHER, V. Motorishe funktion des tectal und tegmental gebietes. *Monatsschr. Psychiatr. Neurol.* 112: 1–52, 1946.

HIKOSAKA, O. AND WURTZ, R. H. Modification of saccadic eye movements by GABA-related substances. I. Effect of muscimol and bicuculline in monkey superior colliculus. *J. Neurophysiol.* 53: 266–291, 1985.

HIKOSAKA, O. AND WURTZ, R. H. Saccadic eye movements following injection of lidocaine into the superior colliculus. *Exp. Brain Res.* 61: 531–539, 1986.

JURGENS, R., BECKER, W., AND KORNHUBER, H. H. Natural and drug-induced variations of velocity and duration of human saccadic eye movements: evidence for a control of the neural pulse generator by local feedback. *Biol. Cybern.* 39: 87–96, 1981.

KELLER, E. L. Participation of medial pontine reticular formation in eye movement generation in monkey. *J. Neurophysiol.* 37: 316–332, 1974.

KELLER, E. L. Colliculoreticular organization in the oculomotor system. *Prog. Brain Res.* 50: 725–734, 1979.

KELLER, E. L. Brain stem mechanisms in saccadic control. In: *Progress in Oculomotor Research*, edited by A. F. Fuchs and W. Becker. Amsterdam: Elsevier/North-Holland, 1981, p. 57–62.

KING, W. M., PRECHT, W., AND DIERINGER, W. Afferent and efferent connections of cat omnipause neurons. *Exp. Brain Res.* 38: 395–403, 1980.

LEE, C., ROHRER, W. H., AND SPARKS, D. L. Population coding of saccadic eye movements by neurons in the superior colliculus. *Nature Lond.* 332: 357–360, 1988.

LEFEVRE, P. AND GALIANA, H. L. Velocity versus position feedback to the superior colliculus in gaze control modelling. *Soc. Neurosci. Abstr.* 16: 1084, 1990.

LUSCHEI, E. S. AND FUCHS, A. F. Activity of brain stem neurons during eye movements of alert monkeys. *J. Neurophysiol.* 35: 445–461, 1972.

LYNCH, J. C., GRAYBIEL, A. M., AND LOBECK, L. J. The differential projection of two cytoarchitectonic subregions of the inferior parietal lobule of macaque upon the deep layers of the superior colliculus. *J. Comp. Neurol.* 235: 241–254, 1985.

LYNCH, J. C., MOUNTCASTLE, V. B., TALBOT, W. H., AND YIN, T. C. T. Parietal lobe mechanisms for directed visual attention. *J. Neurophysiol.* 40: 362–386, 1977.

MAYS, L. E. AND SPARKS, D. L. Dissociation of visual and saccade-related responses in superior colliculus neurons. *J. Neurophysiol.* 43: 207–232, 1980.

MCCREA, R. A., STRASSMAN, A., AND HIGHSTEIN, S. M. Anatomical and physiological characteristics of vestibular neurons mediating the vertical vestibulo-ocular reflexes of the squirrel monkey. *J. Comp. Neurol.* 264: 571–594, 1987.

MCILWAIN, J. T. Visual receptive fields and their images in superior colliculus of the cat. *J. Neurophysiol.* 38: 219–230, 1975.

MCILWAIN, J. T. Lateral spread of neural excitation during microstimulation in intermediate gray layer of cat's superior colliculus. *J. Neurophysiol.* 47: 167–178, 1982.

MCILWAIN, J. T. Point images in the visual system: new interest in an old idea. *Trends Neurosci.* 9: 354–358, 1986.

MOHLER, C. W. AND WURTZ, R. H. Organization of monkey superior colliculus: intermediate layer cells discharging before eye movements. *J. Neurophysiol.* 39: 722–744, 1976.

MOSCHOVAKIS, A. K. AND KARABELAS, A. B. Observations on the somatodendritic morphology and axonal trajectory of intracellularly HRP-labeled efferent neurons located in the deeper layers of the superior colliculus of the cat. *J. Comp. Neurol.* 239: 276–308, 1985.

MOSCHOVAKIS, A. K., KARABELAS, A. B., AND HIGHSTEIN, S. M. Structure-function relationships in the primate superior colliculus. I. Morphological classification of efferent neurons. *J. Neurophysiol.* 60: 232–262, 1988a.

MOSCHOVAKIS, A. K., KARABELAS, A. B., AND HIGHSTEIN, S. M. Structure-function relationships in the primate superior colliculus. II. Morphological identity of presaccadic neurons. *J. Neurophysiol.* 60: 263–302, 1988b.

MUNOZ, D. P. *On the Role of the Tecto-Reticulo-Spinal System in Gaze Control* (PhD thesis). Montreal, Canada: McGill University, 1988.

MUNOZ, D. P. AND GUITTON, D. Tectospinal neurons in the cat have discharges coding gaze position error. *Brain Res.* 341: 184–188, 1985.

MUNOZ, D. P. AND GUITTON, D. Presaccadic burst discharges of tecto-reticulo-spinal neurons in the alert head-free and -fixed cat. *Brain Res.* 398: 185–190, 1986.

MUNOZ, D. P. AND GUITTON, D. Fixation and orientation control by the tecto-reticulo-spinal system in the cat whose head is unrestrained. *Rev. Neurol. Paris* 145: 567–579, 1989.

MUNOZ, D. P. AND GUITTON, D. Control of orienting gaze shifts by the tectoreticulospinal system in the head-free cat. II. Sustained discharges during motor preparation and fixation. *J. Neurophysiol.* 66: 1624–1641, 1991.

MUNOZ, D. P., PÉLISSON, D., AND GUITTON, D. Site of neural activity moves on superior colliculus motor map during gaze shifts. *Science Wash. DC* 251: 1358–1360, 1991.

MUNOZ, D. P., WAITZMAN, D. M., AND WURTZ, R. H. Evidence for a fixation zone in the rostral superior colliculus of the monkey. *Soc. Neurosci. Abstr.* 16: 1084, 1990.

PARÉ, M. AND GUITTON, D. Gaze-related activity of brainstem omnipause neurons during combined eye-head gaze shifts in the alert cat. *Exp. Brain Res.* 83: 210–214, 1990.

PECK, C. K. Saccade-related burst neurons in cat superior colliculus. *Brain Res.* 408: 329–333, 1987.

PECK, C. K. Visual responses of neurones in cat superior colliculus in relation to fixation of targets. *J. Physiol. Lond.* 414: 301–315, 1989.

PECK, C. K. Neuronal activity related to head and eye movements in cat superior colliculus. *J. Physiol. Lond.* 421: 79–104, 1990.

PECK, C. K., SCHLAG-REY, M., AND SCHLAG, J. Visuo-oculomotor properties of cells in the superior colliculus of the alert cat. *J. Comp. Neurol.* 194: 97–116, 1980.

PETERSON, B. W. Identification of reticulospinal projections that may participate in gaze control. In: *Control of Gaze by Brain Stem Neurons*, edited by R. Baker and A. Berthoz. Amsterdam: Elsevier/North-Holland, 1977, p. 143–152.

PITTS, W. AND MCCULLOCH, W. S. How we know universals. The perception of auditory and visual forms. *Bull. Math. Biophys.* 9: 127–147, 1947.

RAYBOURN, M. S. AND KELLER, E. L. Colliculoreticular organization in primate oculomotor system. *J. Neurophysiol.* 40: 861–878, 1977.

RICHMOND, B. J., OPTICAN, L. M., PODELL, M., AND SPITZER, H. Temporal encoding of two-dimensional patterns by single units in primate inferior temporal cortex. I. Response characteristics. *J. Neurophysiol.* 57: 132–146, 1987.

ROBINSON, D. A. Oculomotor control signals. In: *Basic Mechanisms of Ocular Motility and Their Clinical Implications*, edited by G. Lennerstrand and P. Bach-y-Rita. Oxford, UK: Pergamon, 1975, p. 337–374.

ROBINSON, D. L. AND JARVIS, C. D. Superior colliculus neurons studied during head and eye movements of the behaving monkey. *J. Neurophysiol.* 37: 533–540, 1974.

ROHRER, W. H., WHITE, J. M., AND SPARKS, D. L. Saccade-related burst cells in the superior colliculus: relationship of activity with saccadic velocity. *Soc. Neurosci. Abstr.* 13: 1092, 1987.

ROUCOUX, A., GUITTON, D., AND CROMMELINCK, M. Stimulation of the superior colliculus in the alert cat. II. Eye and head movements evoked when the head is unrestrained. *Exp. Brain Res.* 39: 75–85, 1980.

SAKATA, H., SHIBUTANI, H., AND KAWANO, K. Spatial properties of visual fixation neurons in posterior parietal association cortex of the monkey. *J. Neurophysiol.* 43: 1654–1672, 1980.

SCHILLER, P. H. AND KOERNER, F. Discharge characteristics of single units

in superior colliculus of the alert rhesus monkey. *J. Neurophysiol.* 34: 920–936, 1971.

SCHILLER, P. H., SANDELL, J. H., AND MAUNSELL, J. H. R. The effect of frontal eye field and superior colliculus lesions on saccade latencies in the rhesus monkey. *J. Neurophysiol.* 57: 1033–1049, 1987.

SCHILLER, P. H. AND STRYKER, M. Single-unit recording and stimulation in superior colliculus of the alert rhesus monkey. *J. Neurophysiol.* 35: 915–924, 1972.

SCHILLER, P. H., TRUE, S. D., AND CONWAY, J. L. Deficits in eye movements following frontal eye field and superior colliculus ablations. *J. Neurophysiol.* 44: 1175–1189, 1980.

SCUDDER, C. A. A new local feedback, model of the saccadic burst generator. *J. Neurophysiol.* 59: 1455–1475, 1988.

SCUDDER, C. A., HIGHSTEIN, S., KARABELAS, T., AND MOSCHOVAKIS, A. Anatomy and physiology of long-lead burst neurons (LLBNs). *Soc. Neurosci. Abstr.* 15: 238, 1989.

SEGRAVES, M. A. AND GOLDBERG, M. E. Functional properties of corticotectal neurons in the monkey's frontal eye field. *J. Neurophysiol.* 58: 1387–1419, 1987.

SILVERMAN, B. W. *Density Estimation for Statistics and Data Analysis.* London: Chapman and Hall, 1986.

SPARKS, D. L. Response properties of eye movement-related neurons in the monkey superior colliculus. *Brain Res.* 90: 147–152, 1975.

SPARKS, D. L. Functional properties of neurons in the monkey superior colliculus: coupling of neuronal activity and saccade onset. *Brain Res.* 156: 1–16, 1978.

SPARKS, D. L., HOLLAND, R., AND GUTHRIE, B. L. Size and distribution of movement fields in the monkey superior colliculus. *Brain Res.* 113: 21–34, 1976.

SPARKS, D. L. AND MAYS, L. E. Movement fields of saccade-related burst neurons in the monkey superior colliculus. *Brain Res.* 190: 39–50, 1980.

SPARKS, D. L. AND MAYS, L. E. The role of the monkey superior colliculus in the control of saccadic eye movements: a current perspective. In: *Progress in Oculomotor Research,* edited by A. F. Fuchs and W. Becker, Amsterdam: Elsevier/North-Holland, 1981, p. 137–144.

SPARKS, D. L. AND MAYS, L. E. Spatial localization of saccade targets. I. Compensation for stimulation-induced perturbations in eye position. *J. Neurophysiol.* 49: 45–63, 1983.

STRASCHILL, M. AND SCHICK, F. Discharges of superior colliculus neurons during head and eye movements of the alert cat. *Exp. Brain Res.* 27: 131–141, 1977.

STRASSMAN, A., HIGHSTEIN, S. M., AND MCCREA, R. A. Anatomy and physiology of saccadic burst neurons in the alert squirrel monkey. 1. Excitatory burst neurons. *J. Comp. Neurol.* 249: 337–357, 1986.

SYKA, J. AND RADIL-WEISS, T. Electrical stimulation of the tectum in freely moving cats. *Brain Res.* 28: 567–572, 1972.

TOMLINSON, R. D. AND BAHRA, P. S. Combined eye-head gaze shifts in the primate. I. Metrics. *J. Neurophysiol.* 56: 1542–1557, 1986.

TWEED, D. AND VILIS, T. A two dimensional model for saccade generation. *Biol. Cybern.* 52: 219–227, 1985.

TWEED, D. AND VILIS, T. The superior colliculus and spatio temporal translation in the saccadic system. *Neural Networks* 3: 75–86, 1990.

VAN GISBERGEN, J. A. M., VAN OPSTAL, A. J., AND TAX, A. A. M. Collicular ensemble coding of saccades based on vector summation. *Neuroscience* 21: 541–555, 1987.

VAN OPSTAL, A. J. AND VAN GISBERGEN, J. A. M. Role of monkey superior colliculus in saccade averaging. *Exp. Brain Res.* 79: 143–149, 1990.

WAITZMAN, D. M., MA, T. P., OPTICAN, L. M., AND WURTZ, R. H. Superior colliculus neurons provide the saccadic motor error signal. *Exp. Brain Res.* 72: 649–652, 1988.

WURTZ, R. H. AND GOLDBERG, M. E. Superior colliculus cell responses related to eye movements in awake monkeys. *Science Wash. DC* 171: 82–84, 1971.

WURTZ, R. H. AND GOLDBERG, M. E. Activity of superior colliculus in behaving monkey. III. Cells discharging before eye movements. *J. Neurophysiol.* 35: 575–586, 1972a.

WURTZ, R. H. AND GOLDBERG, M. E. Activity of superior colliculus in behaving monkey. IV. Effects of lesions on eye movements. *J. Neurophysiol.* 35: 587–596, 1972b.